Combined Analysis: NPD-XRD (Texture, residual stress …) – XRF – Raman, and Magnetic QTA ?

D. Chateigner, L. Lutterotti

Normandie Université, Univ. Trento

Normandie Université

SOLSA

UNIVERSITÀ DEGLI STUDI DI TRENTO

ENSICAEN

IUT CAEN

UNICAEN

ILL, Grenoble, France, 7th Mar. 2019

Scattering "sees"

Texture
$f(g)_{\Phi,L}$

Structure
$|F_{\mathbf{h}}|^2_{\Phi,L}$

Real samples
Layered samples
thicknesses
roughnesses
$\rho(z)$…

Residual Stress
$<C_{ijkl}(g)>_{\Phi,L}$

Raman, IR

Phase ID

Phase
$S_{\Phi,L}$

Element ID

XRF

defects (0D .. nD)
broadening
asymmetry

Why not benefit of texture in Structure determination ?

Perfect powders:
- overlaps (intra- and inter-p
- no angular constrain
- anisotropy difficult to resc

Single pattern

Single crystals:
- reduced overlaps
- max angular constrains
- Perfect texture: max anisotropy

Many individual diffracted peaks

Textured powders:
- reduced overlaps
- angular constrain = f(texture strength)
- Intermediate anisotropy

Many patterns to measure and analyse

Rietveld: extended to lots of spectra

$$y_c(\mathbf{y}_S,\theta,\eta) = y_b(\mathbf{y}_S,\theta,\eta) + I_0 \sum_{i=1}^{N_L} \sum_{\Phi=1}^{N_\Phi} \frac{\nu_{i\Phi}}{V_{c\Phi}^2} \sum_h Lp(\theta) j_{\Phi h} \left|F_{\Phi h}\right|^2 \Omega_{\Phi h}(\mathbf{y}_S,\theta,\eta) P_{\Phi h}(\mathbf{y}_S,\theta,\eta) A_{i\Phi}(\mathbf{y}_S,\theta,\eta)$$

Texture:

$$P_h(\mathbf{y}_S) = \int_{\tilde{\varphi}} f(g,\tilde{\varphi})\, d\tilde{\varphi}$$

E-WIMV, components, Harmonics, Exp. Harmonics …

Strain-Stress:

$$\langle S \rangle_{geo}^{-1} = \left[\prod_{m=1}^{N} S_m^{\nu_m}\right]^{-1} = \prod_{m=1}^{N} S_m^{-\nu_m} = \prod_{m=1}^{N} \left(S_m^{-1}\right)^{\nu_m} = \left\langle S^{-1} \right\rangle_{geo} = \langle C \rangle_{geo}$$

Geometric mean, Voigt, Reuss, Hill …

Layering:

$$A_{i\Phi} = \frac{\nu_{i\Phi} \sin\theta_i \sin\theta_o}{\bar{\mu}_i (\sin\theta_i + \sin\theta_o)} \left\{1 - e^{-\bar{\mu}_i \tau_i W}\right\} \prod_{k<i} e^{-\bar{\mu}_k \tau_k W}$$

$$W = \frac{1}{\sin\theta_i} + \frac{1}{\sin\theta_o}$$

Stacks, coatings, multilayers …

Line Broadening:

Popa, Delft: Crystallite sizes, shapes, microstrains, distributions
0D-3D defects

X-Ray Reflectivity (specular):

Matrix, Parrat, DWBA, EDP …

X-Ray Fluorescence/GiXRF:

De Boer

Electron Diffraction Patterns:

2-waves Blackman

Line Broadening:

Crystallite sizes, shapes, μstrains, distributions

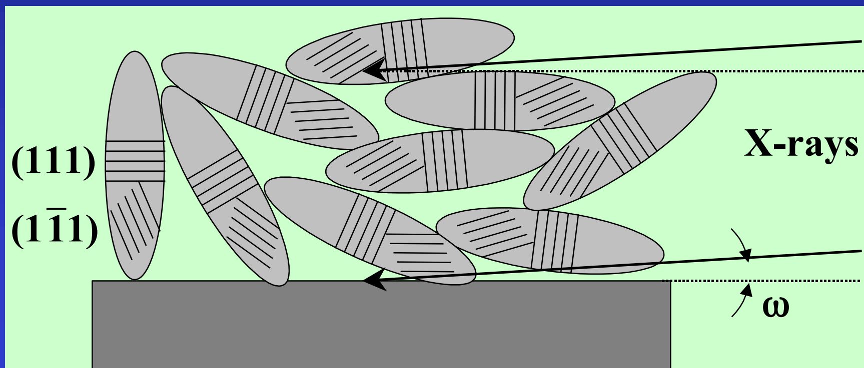

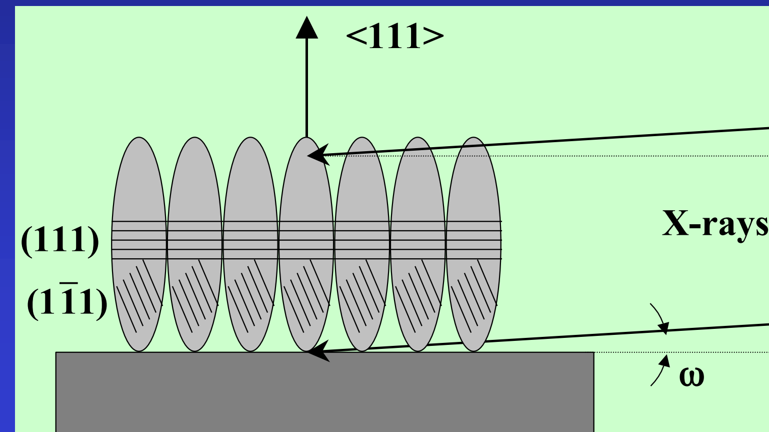

- Texture helps the "real" mean shape determination

$$\left\langle R_{\vec{h}} \right\rangle = \sum_{\ell=0}^{L} \sum_{m=0}^{\ell} R_\ell^m K_\ell^m(\chi, \varphi)$$

Symmetrised spherical harmonics

$$K_\ell^m(\chi, \varphi) = P_\ell^m(\cos\chi)\cos(m\varphi) + P_\ell^m(\cos\chi)\sin(m\varphi)$$

$$\langle R_{\mathbf{h}} \rangle = R_0 + R_1 P_2^{\,0}(x) + R_2 P_2^{\,1}(x)\cos\varphi + R_3 P_2^{\,1}(x)\sin\varphi + R_4 P_2^{\,2}(x)\cos 2\varphi + R_5 P_2^{\,2}(x)\sin 2\varphi + \ldots$$

$$\langle \varepsilon_{\mathbf{h}}^{\,2} \rangle E_{\mathbf{h}}^{\,4} = E_1 h^4 + E_2 k^4 + E_3 \ell^4 + 2E_4 h^2 k^2 + 2E_5 \ell^2 k^2 + 2E_6 h^2 \ell^2 + 4E_7 h^3 k + 4E_8 h^3 \ell + 4E_9 k^3 h + 4E_{10} k^3 \ell + 4E_{11} \ell^3 h + 4E_{12} \ell^3 k + 4E_{13} h^2 k \ell + 4E_{14} k^2 h \ell + 4E_{15} \ell^2 k h$$

$\bar{1}$

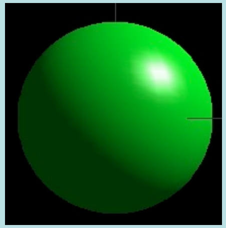

R_0

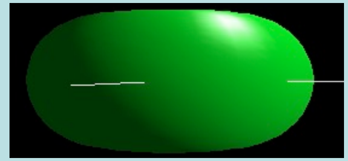

R_0, $R_1 < 0$

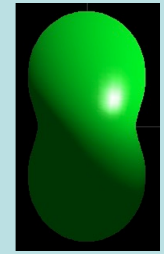

R_0, $R_1 > 0$

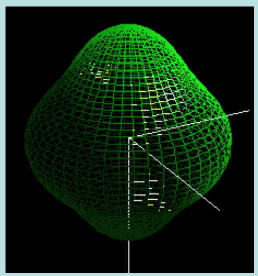

R_0, $R_6 > 0$

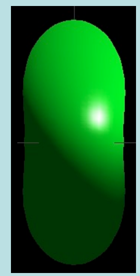

R_0,
R_2 and $R_6 > 0$

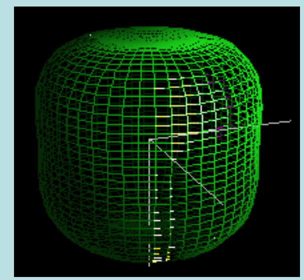

R_0, $R_6 < 0$

6/m

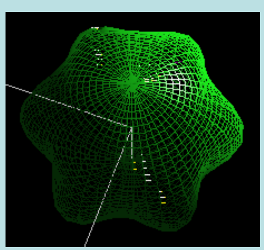

R_0, $R_4 > 0$

m3m

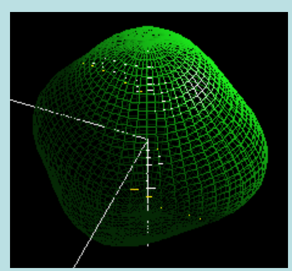

R_0, $R_1 > 0$

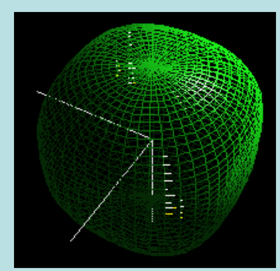

R_0, $R_1 < 0$

EMT nanocrystalline zeolite

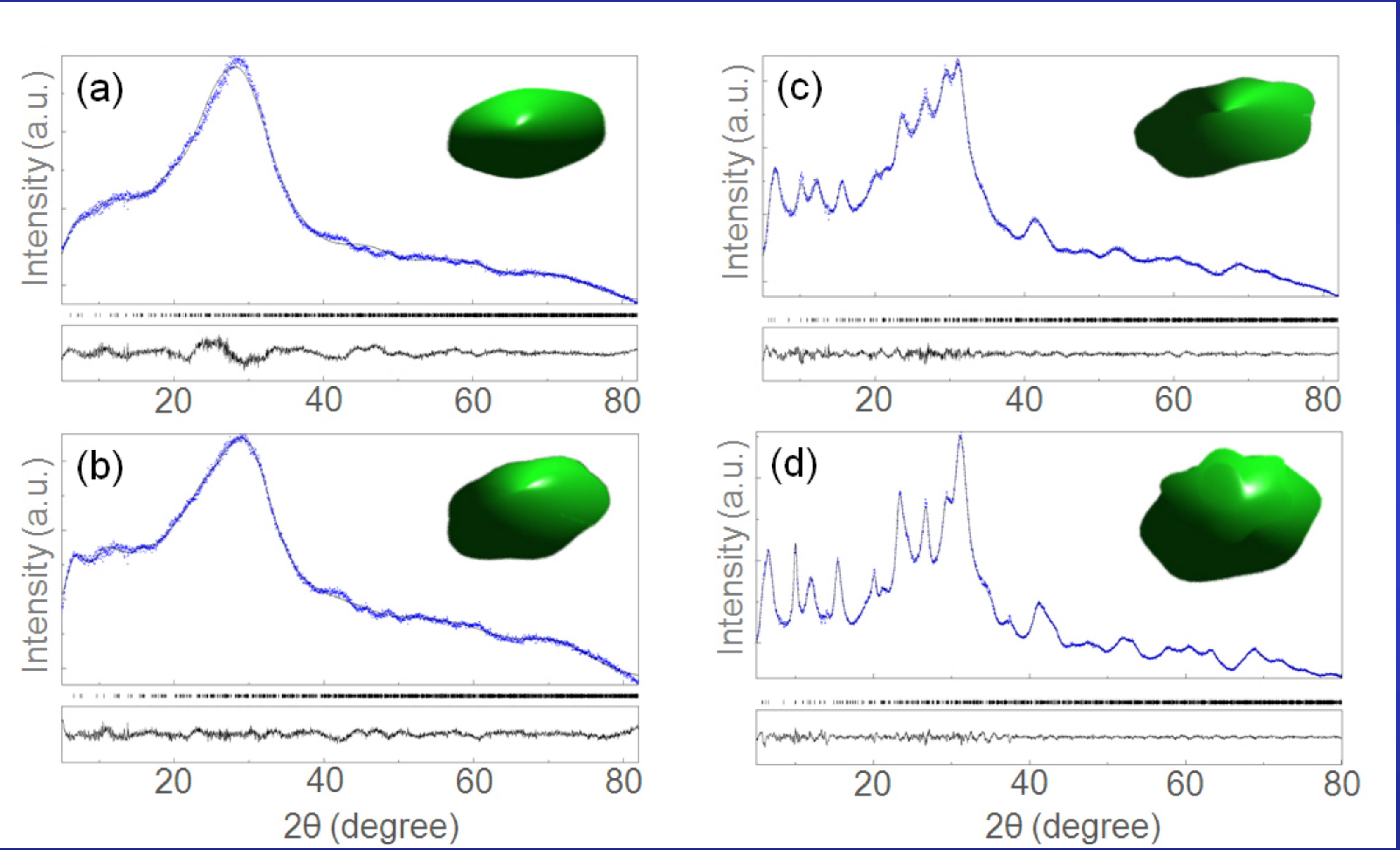

Ng, Chateigner, Valtchev, Mintova: *Science* **335** (2012) 70

Combined Analysis approach

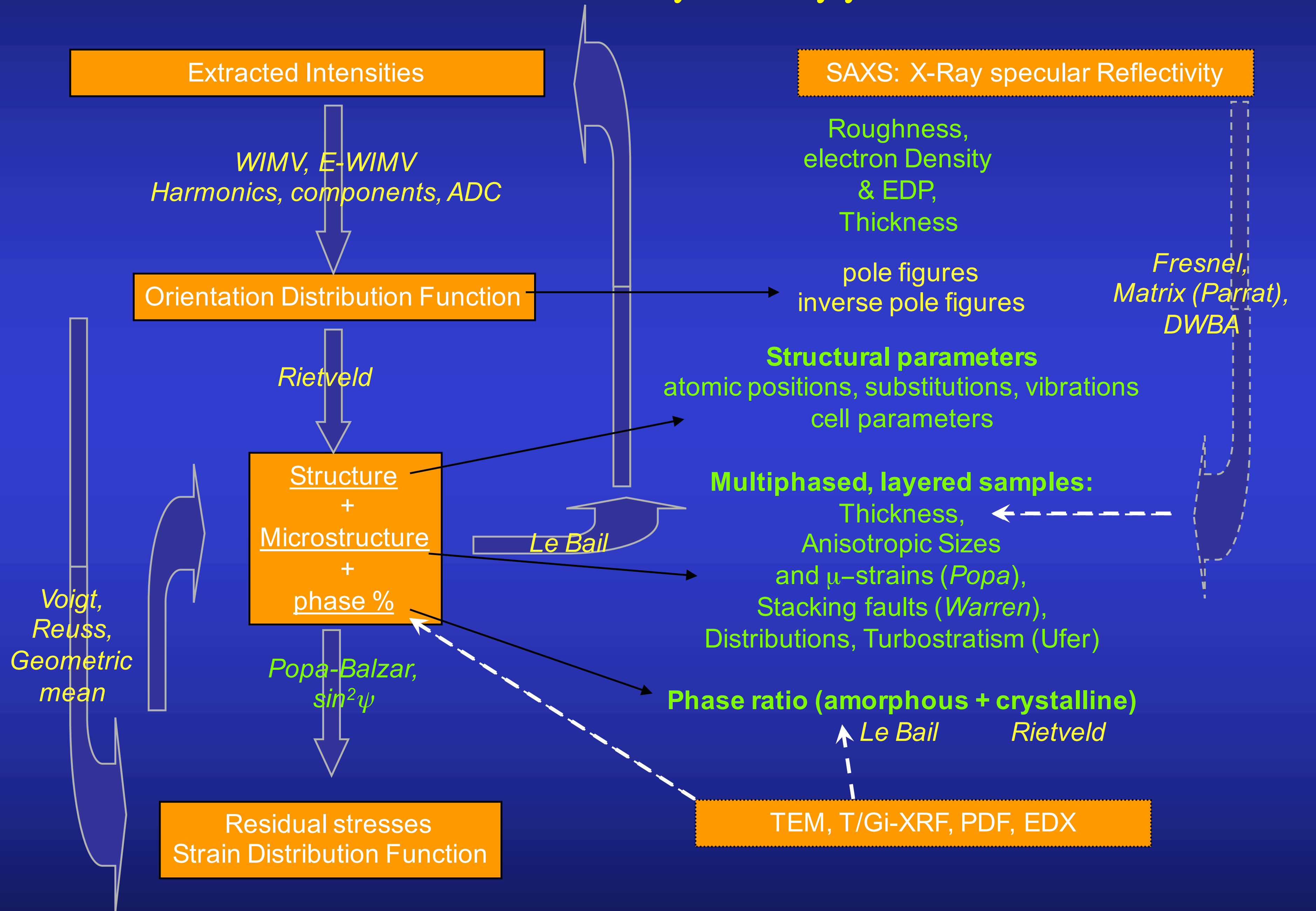

Minimum experimental requirements

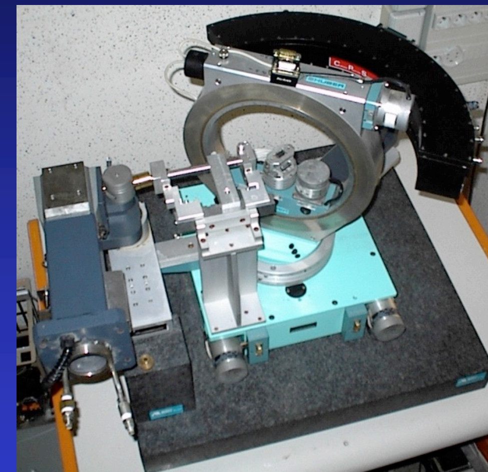

1D or 2D Detector + 4-circle diffractometer
(X-rays and neutrons)
CRISMAT, ILL (B. Ouladdiaf, T. Hansen)

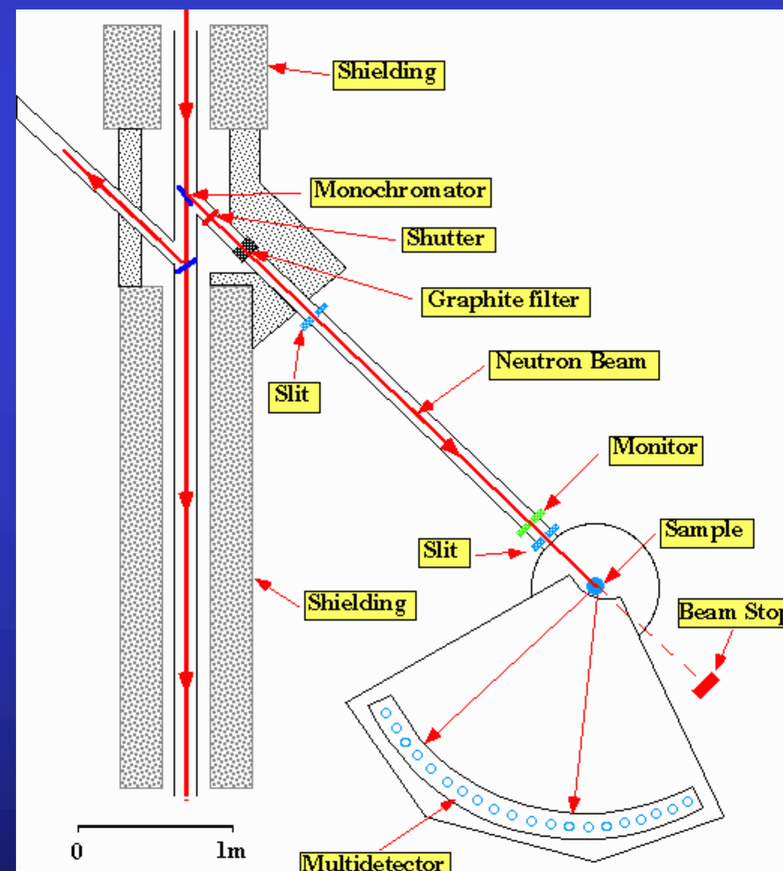

+

~1000 experiments (2θ diagrams)
in as many sample orientations

+

Instrument calibration
(peaks widths and shapes,
misalignments, defocusing …)

2D Curved Area Position Sensitive Detector

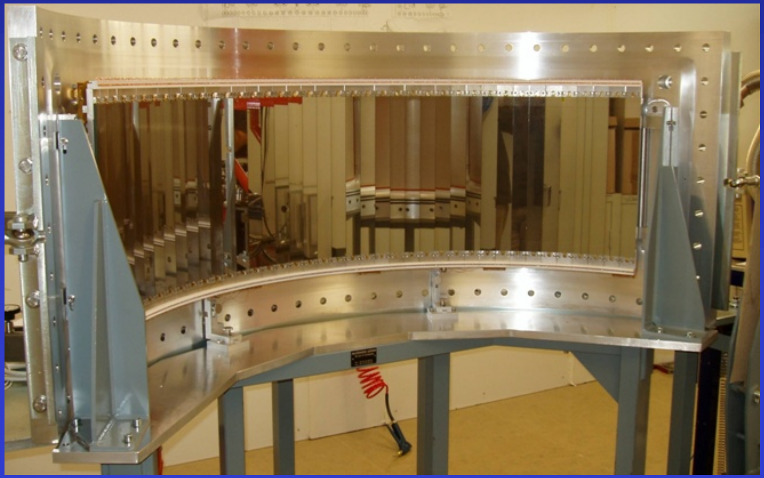

D19 - ILL

+

~100 experiments (2D Debye-Scherrer diagrams)
in as many sample orientations

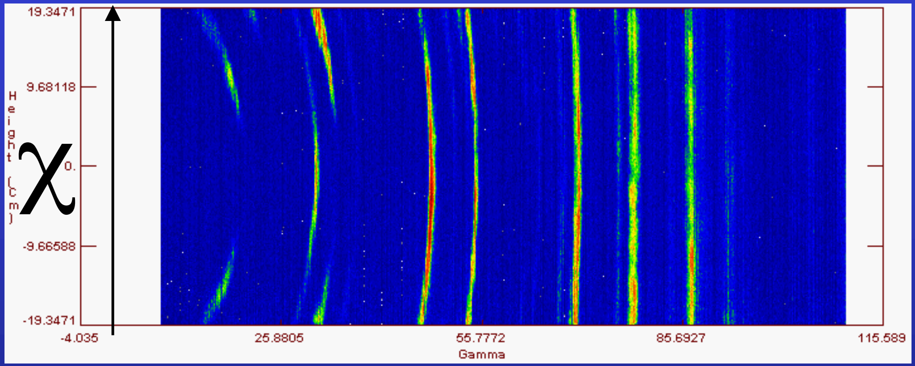

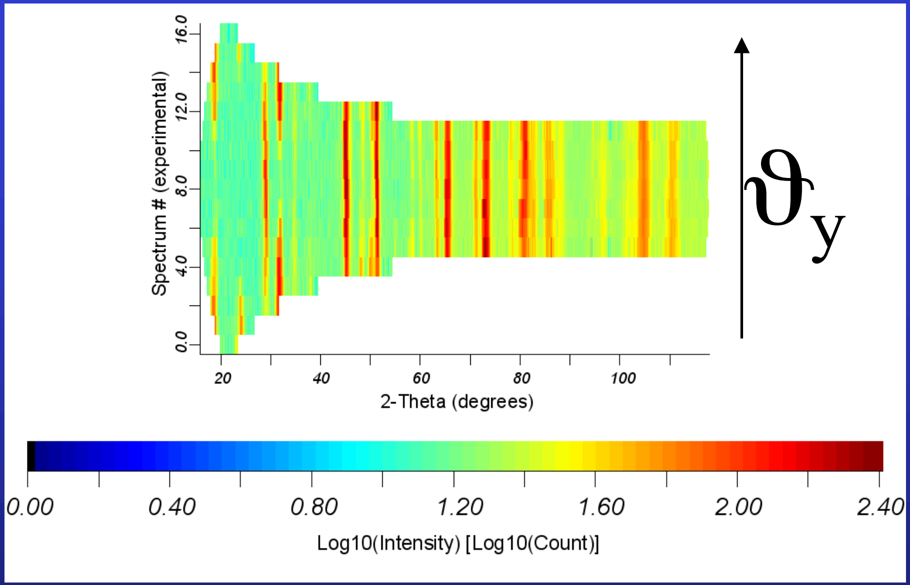

Minimum experimental requirements

1D or 2D Detector +
4-circle diffractometer
(CRISMAT – ANR EcoCorail)

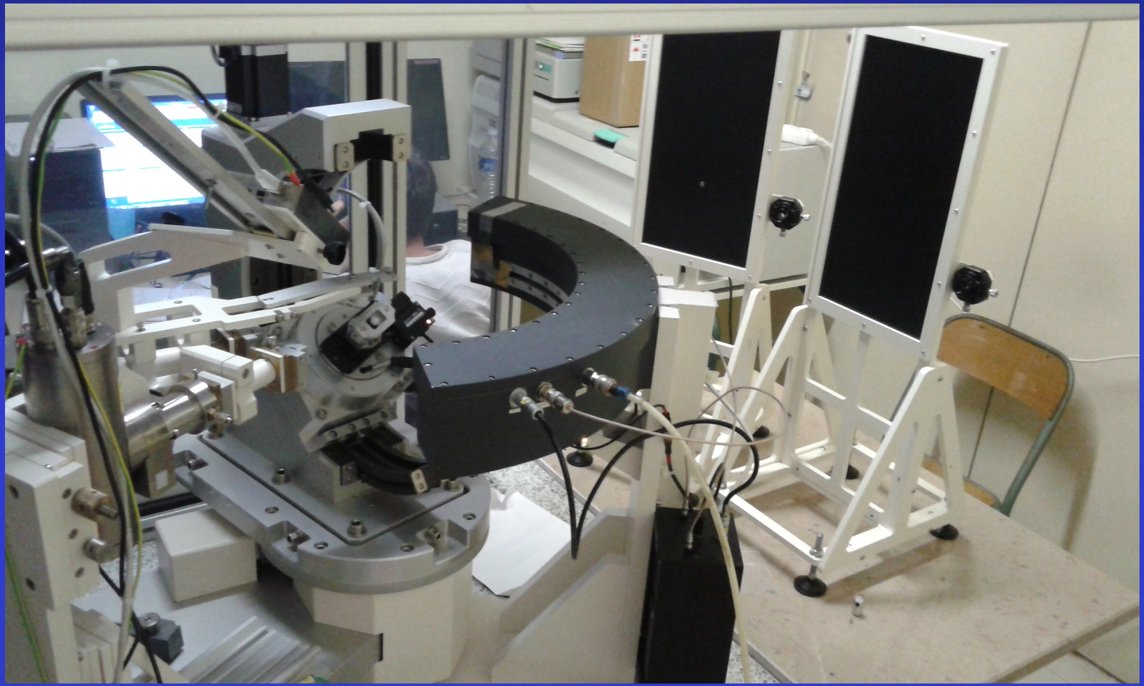

~1000 experiments (2θ diagrams)
in as many sample orientations

+

Instrument calibration
(peaks widths and shapes,
misalignments, defocusing …)

Independent measurements

Different wavelengths and rays

Reflectivity: thickness, roughness, electron density profiles

X-ray Fluorescence: composition

Spectroscopies: local structures (PDF, FTIR, Mossbauer …), eventually anisotropic (P-EXAFS, ESR, Raman …), Element profiles (SIMS, RBS …) …

Physical models: magnetisation, conductivity …

Environments: applied fields

Combined Analysis cost function

$$WSS = \sum_{t=1}^{N_p} u_t \sum_{i=0}^{N_t} w_{it} \left(y_{itc} - y_{ito} \right)^2$$

For each pattern t: w_{it} : weight, usually $1/y_i = \sigma^2$.

u_t : weight of each pattern set t
should be used to adjust the importance we want to give to a particular technique or pattern set with respect to the others

Grinding-Spinning to powderise another problem !

Grinding: removes angular relationship, adds correlations

Spinning: what if the fiber texture axis // spinning axis ?

Texture and strains:
- not measured, not removed ?
- added ?

Same sample ? Rare samples ?
Impossible to grind ?

Correction: without measuring it ? (March-Dollase)

$Ca_3Co_4O_9$ thermoelectrics

$Ca_3Co_4O_9$: Misfit lamellar and modulated Structure, with high thermopower

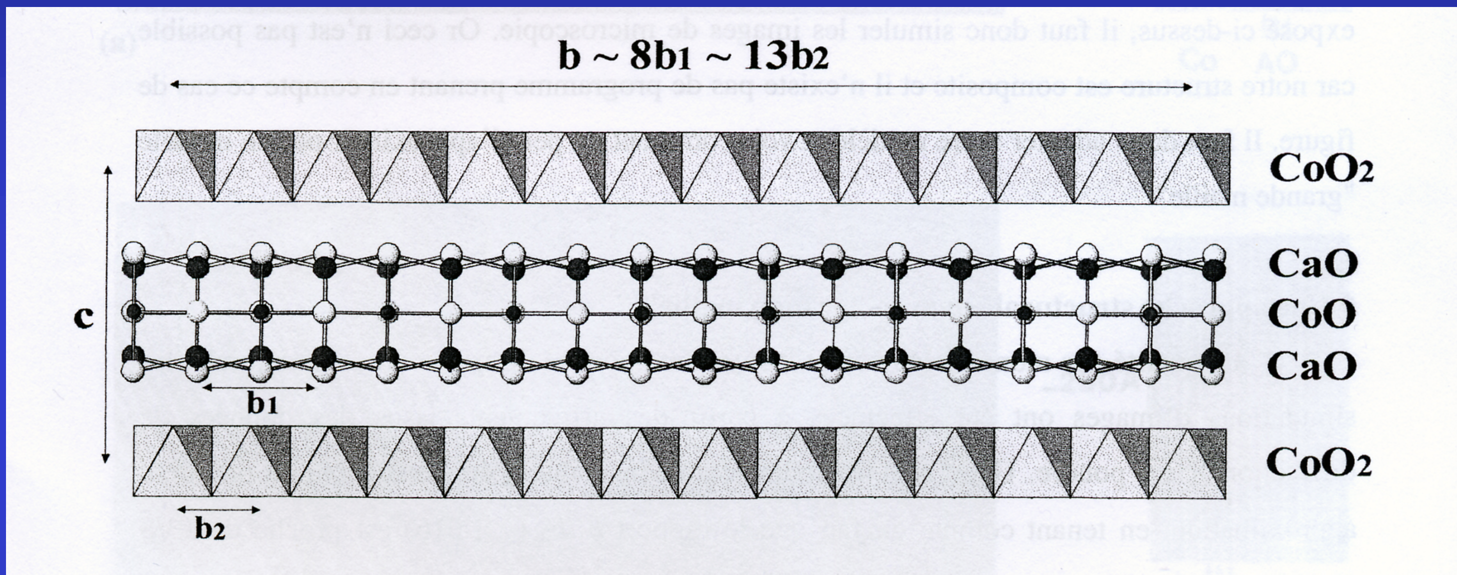

Two monoclinic sub-systems:
S1 with a ~ 4.8Å, b_1 ~ 4.5Å, c ~ 10.8Å et β ~ 98° (NaCl-type
S2 with a ~ 4.8Å, b_2 ~ 2.8Å, c ~ 10.8Å et β ~ 98° (CdI_2-type)

$\Gamma = \sigma_{ab}/\sigma_c \sim 10$ → Texture

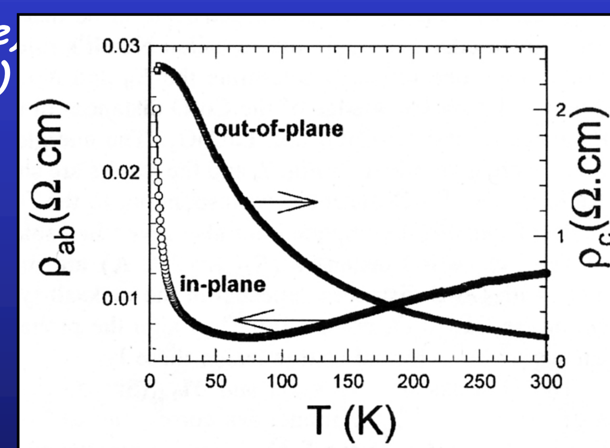

Magnetic alignment + Templated Growth

D. Kenfaui, E. Guilmeau, M. Prevel

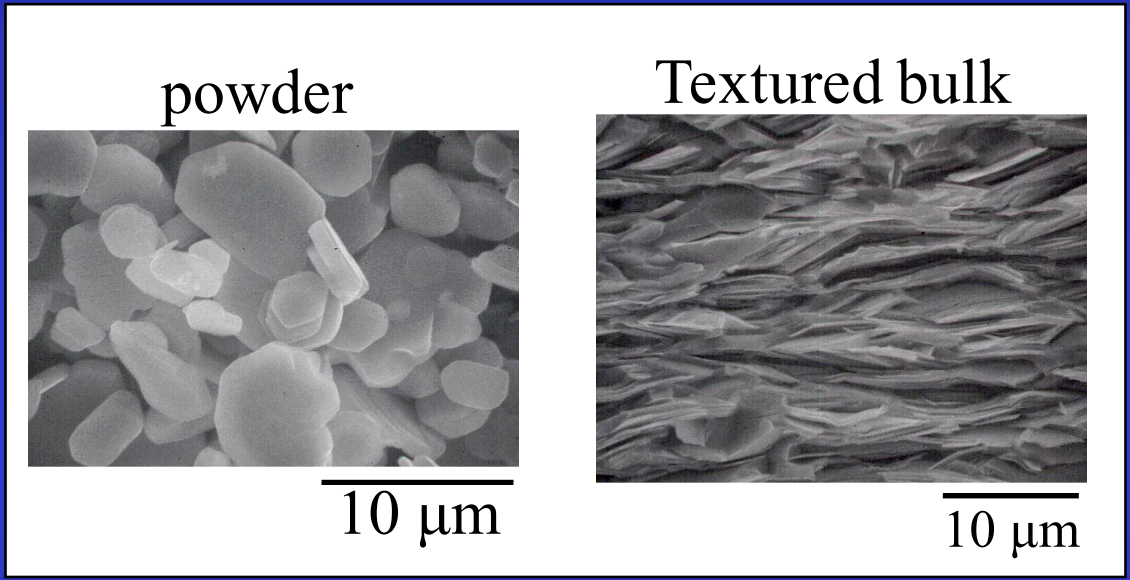

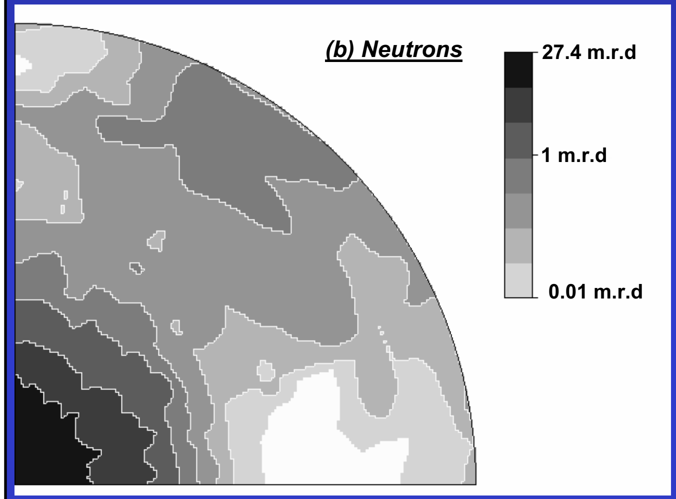

- *Neutrons @D1B*
- *3D Supercell: a=4.8309Å, b~8b1~13b2~36.4902Å, c=10.8353Å, β=98.13°*
174 atoms/cell
- *Sample : 0.6 cm*^{3}

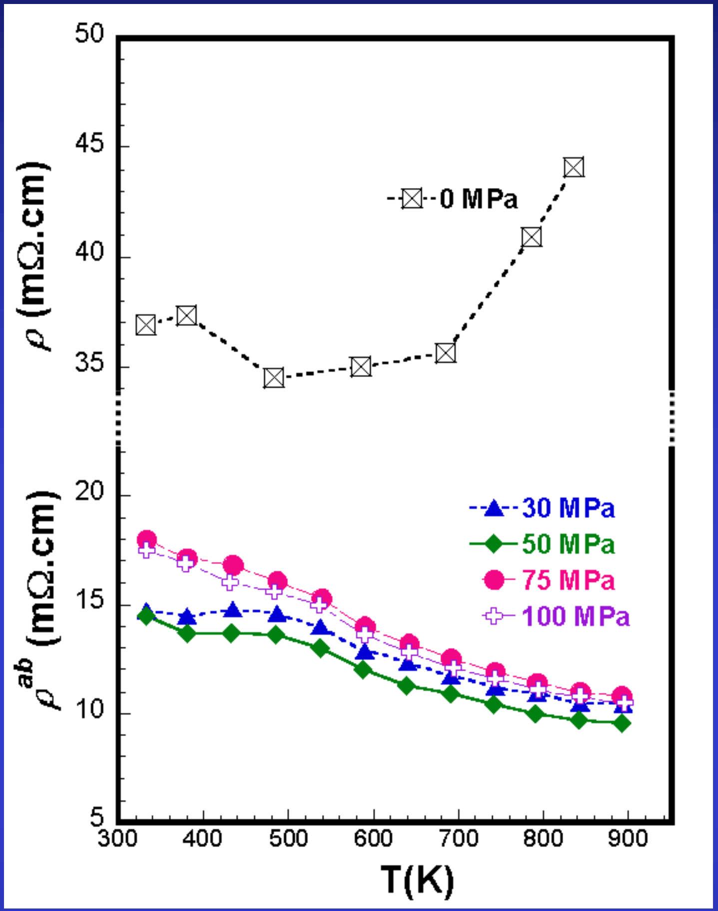

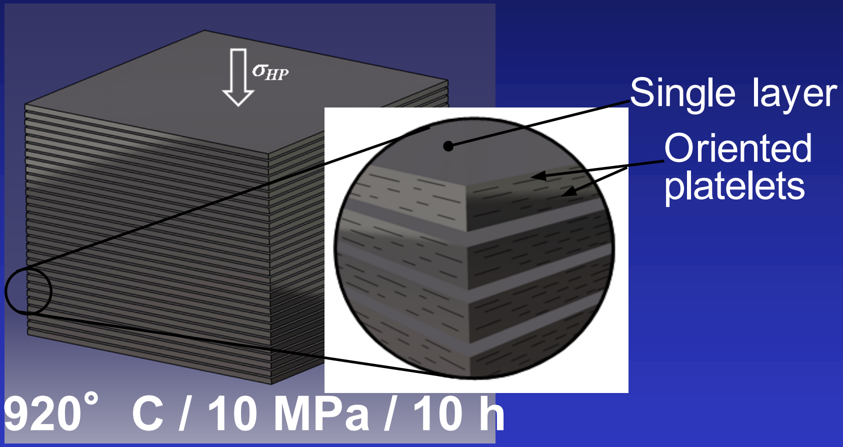

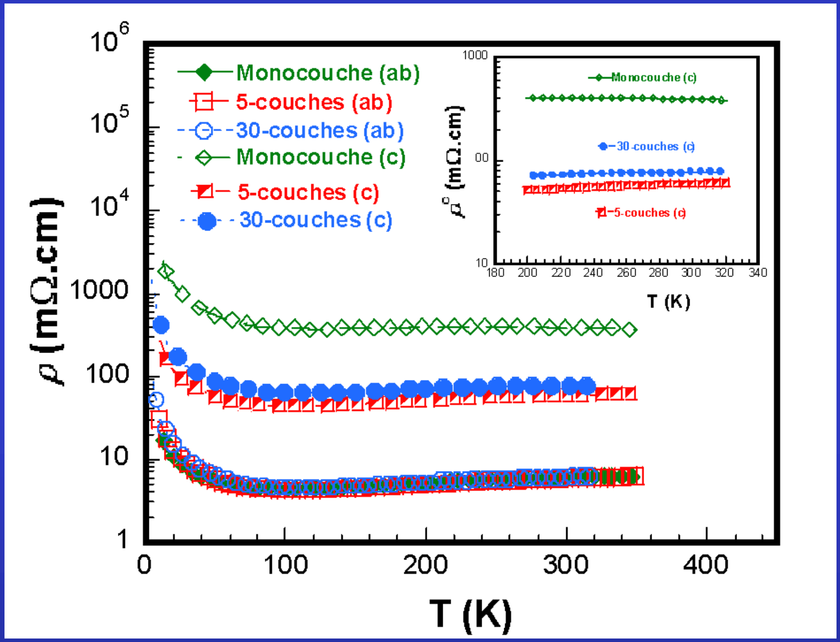

❑ **Texture**

- **neutrons @D1B**
  → volume texture
- **max. {001} : 42.73 mrd**

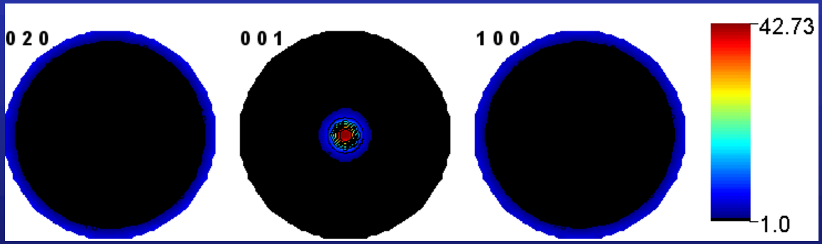

Texture of amphiboles collected at ≠ places and in ≠ lithologic types

M. Zucali, Univ. Milano

↳ **White mica and chlorite partially replace amphibole or fill small fractures with quartz and carbonates**

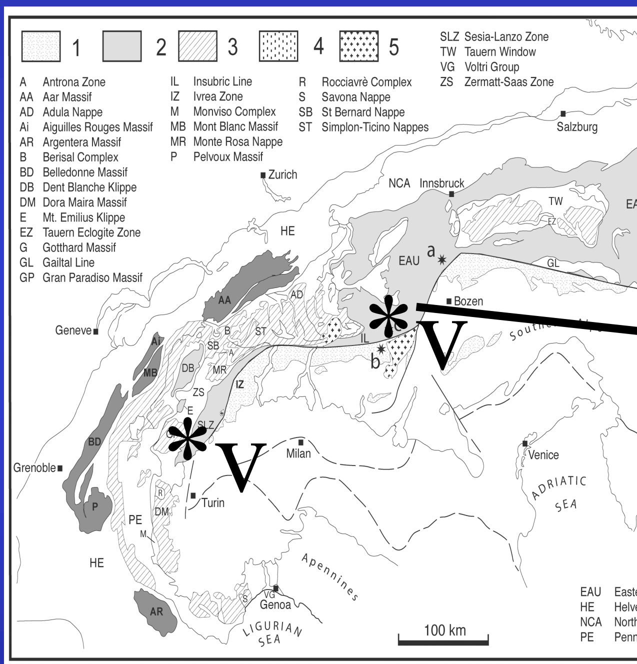

Fig. 1* –Tectonic sketch map of the Alpine chain: shaded areas correspond to continental Alpine crust. Legend: 1 = Southalpine basement; 2 = Austro
4 = Helvetic basement; 5=Tertiary intrusive stocks. Stars localise the Texel Gruppe metapelites in the Oetztal nappe (a), the Eastern Orobic Alps meta
(b) and the Mortirolo Pass area in Central Austroalpine domain of the Languard-Campo Nappe (c).

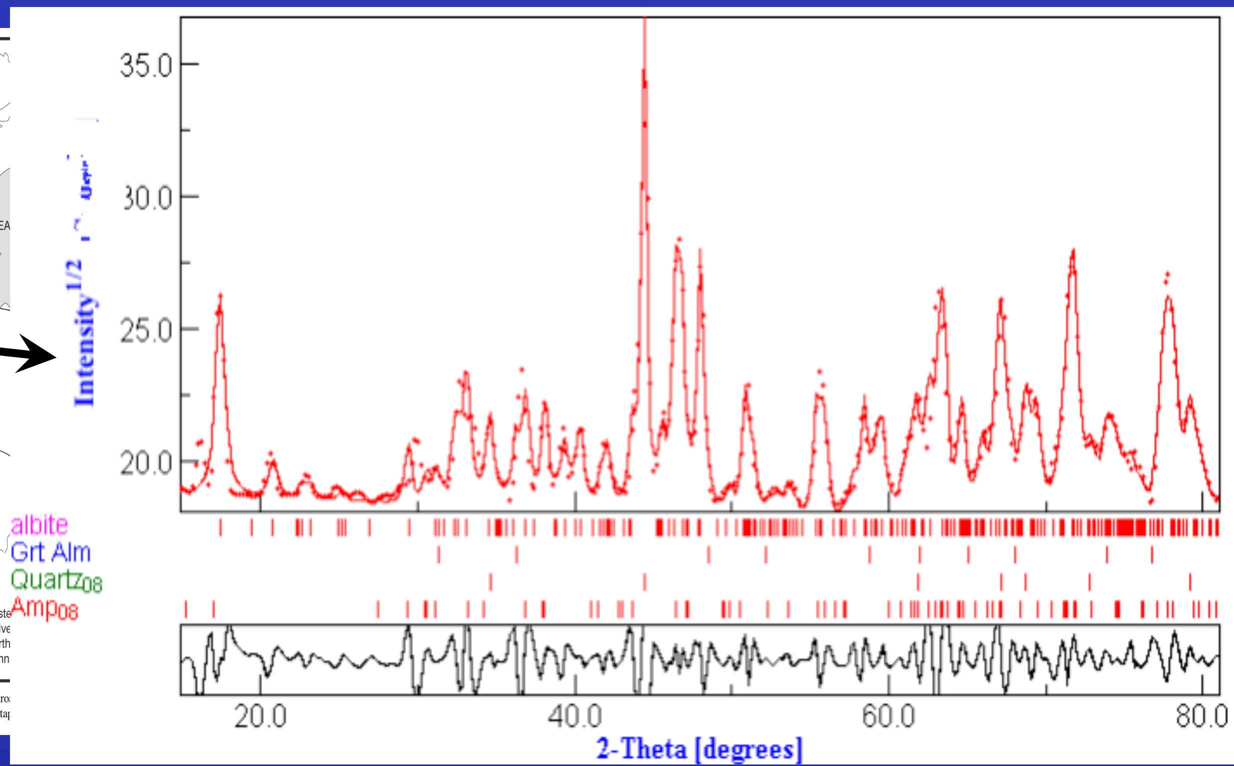

Combined approach allows to access pole figures for most of the rock-forming minerals (even for mica)

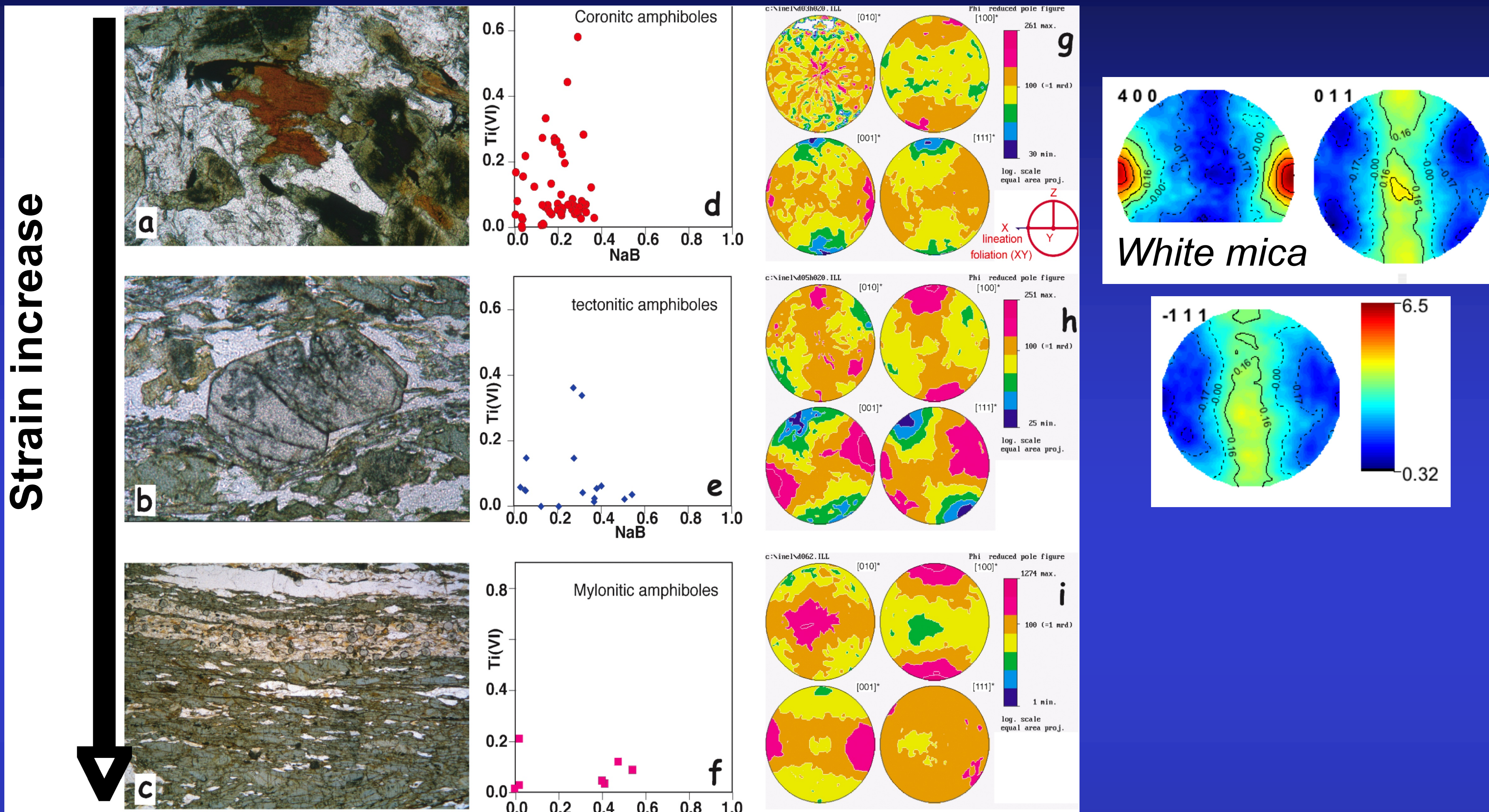

Degree of fabric evolution due to:

- **deformation partitioning at metric-scale**
- **degree of chemical changes within amphiboles**
- **evolving metamorphic conditions during Alpine subduction (60-100 Million years).**

α-Al_2O_3 Slip-casted + magnetically aligned ceramics

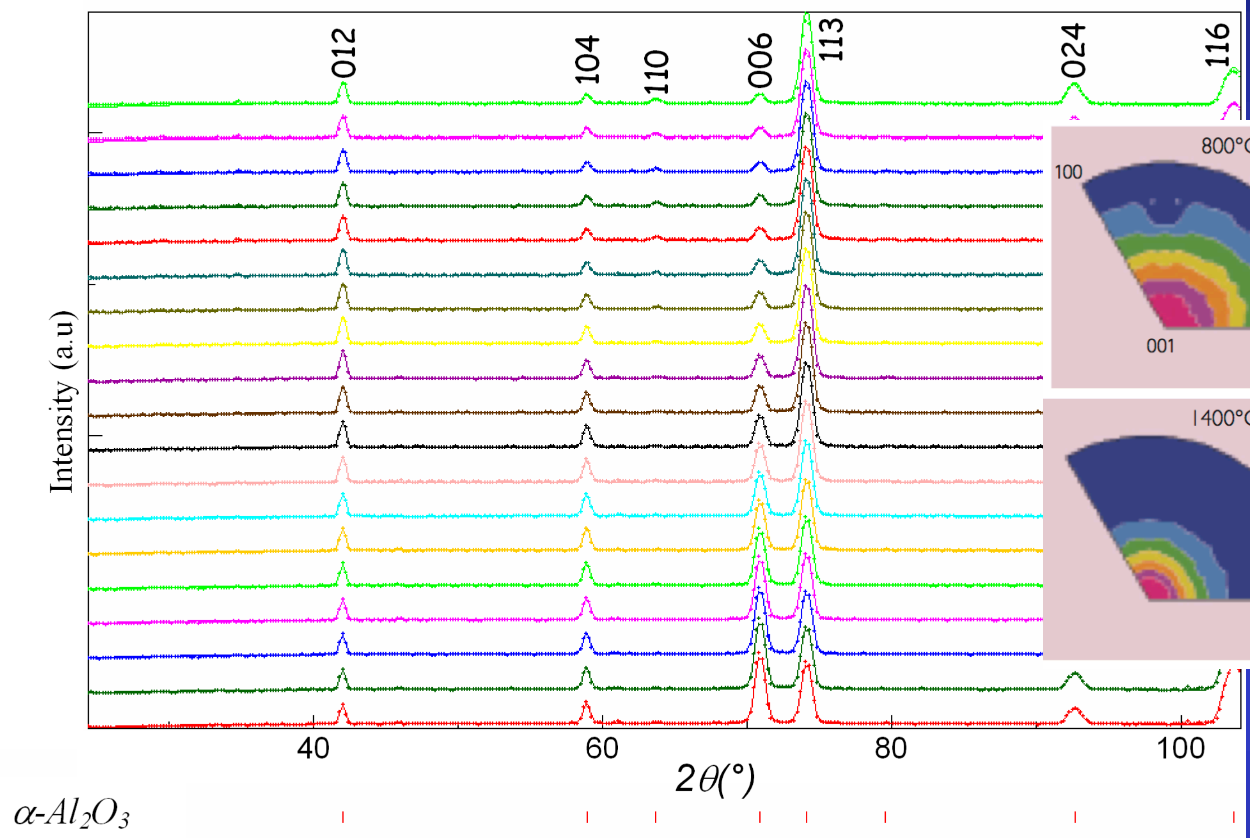

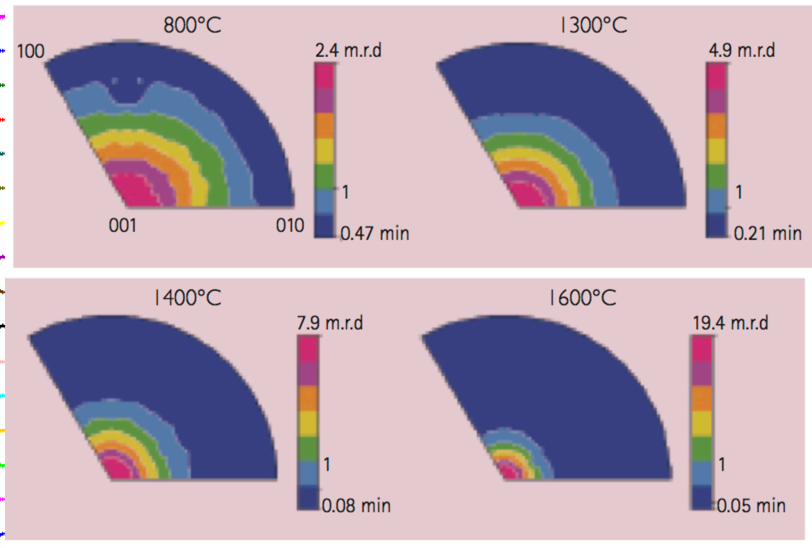

Specimens (Sintering Temperature)	ODF (001) inverse pole figure		Texture Index (F2)	Refined crystallite size (nm)	SEM Calculated grain size (nm)		Aspect Ratio
	Min	Max			$d_{//}$	$d_{\perp}$	$(d_{\perp}/d_{//})$
800°C	0.47	2.4	1.24	137 (13)	~150	~150	1
1300°C	0.21	4.9	2.13	> 1μm	1100	1170	1.063
1400°C	0.08	7.9	3.16	> 1μm	2610	2970	1.138
1600°C	0.05	19.4	7.78	> 1μm	7300	8800	1.205

Carbon nanofibre

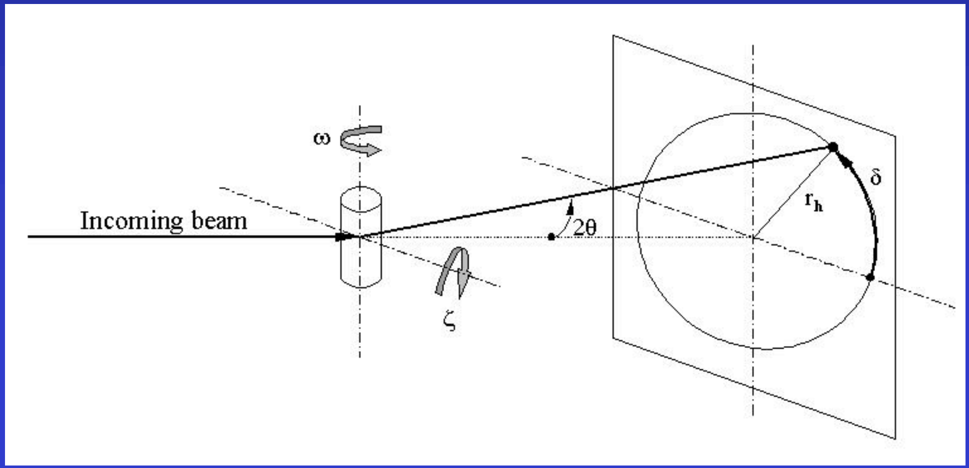

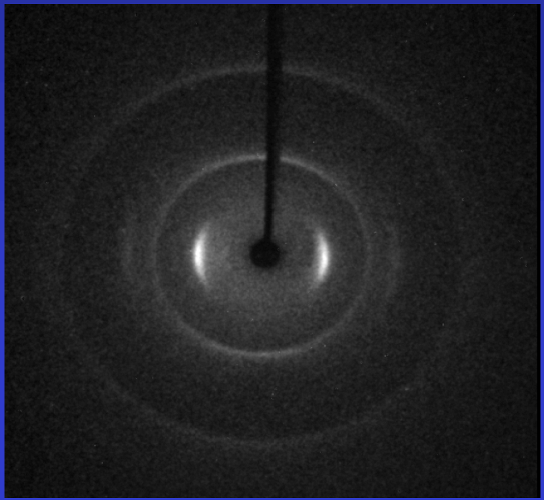

1 fibre (7 microns diameter): CCD Kappa diffractometer

Planar texture Component
Ufer turbostractic model

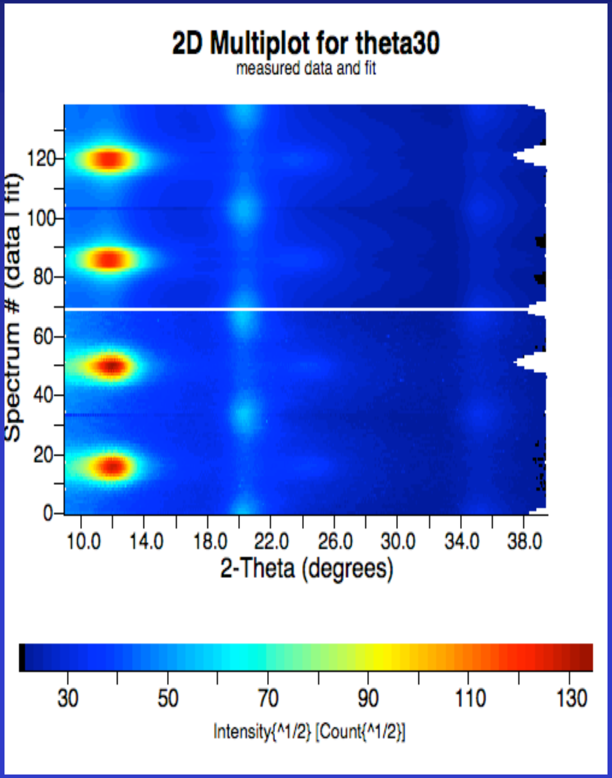

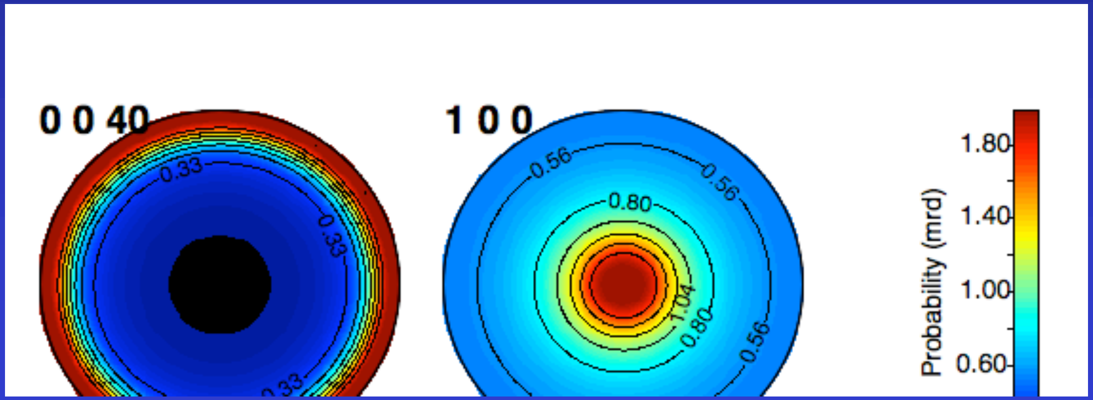

	A(nm)	C(nm)	Orientation FWHM(°)	Max 00l pole figure (m.r.d.)	Crystallite size along c (nm)	Crystallite size along a (nm)	Global microstrain (rms)
C1B1	0.23589(7)	0.6821(1)	21.6(1)	1.95	2.1(4)	2.2(4)	0.0152(10)
C2B1	0.23746(5)	0.68915(8)	18.75(6)	2.05	2.3(2)	2.5(2)	0.0154(11)
C3B1	0.23734(5)	0.69233(9)	18.63(6)	2.04	2.4(3)	2.7(5)	0.0136(6)
C3B2	0.23716(4)	0.69389(9)	19.87(7)	1.98	2.4(4)	2.5(4)	0.0150(4)
C3B3	0.23656(4)	0.68980(8)	19.16(6)	1.99	2.5(6)	2.3(5)	0.0168(8)

Turbostratic phyllosilicate aggregates

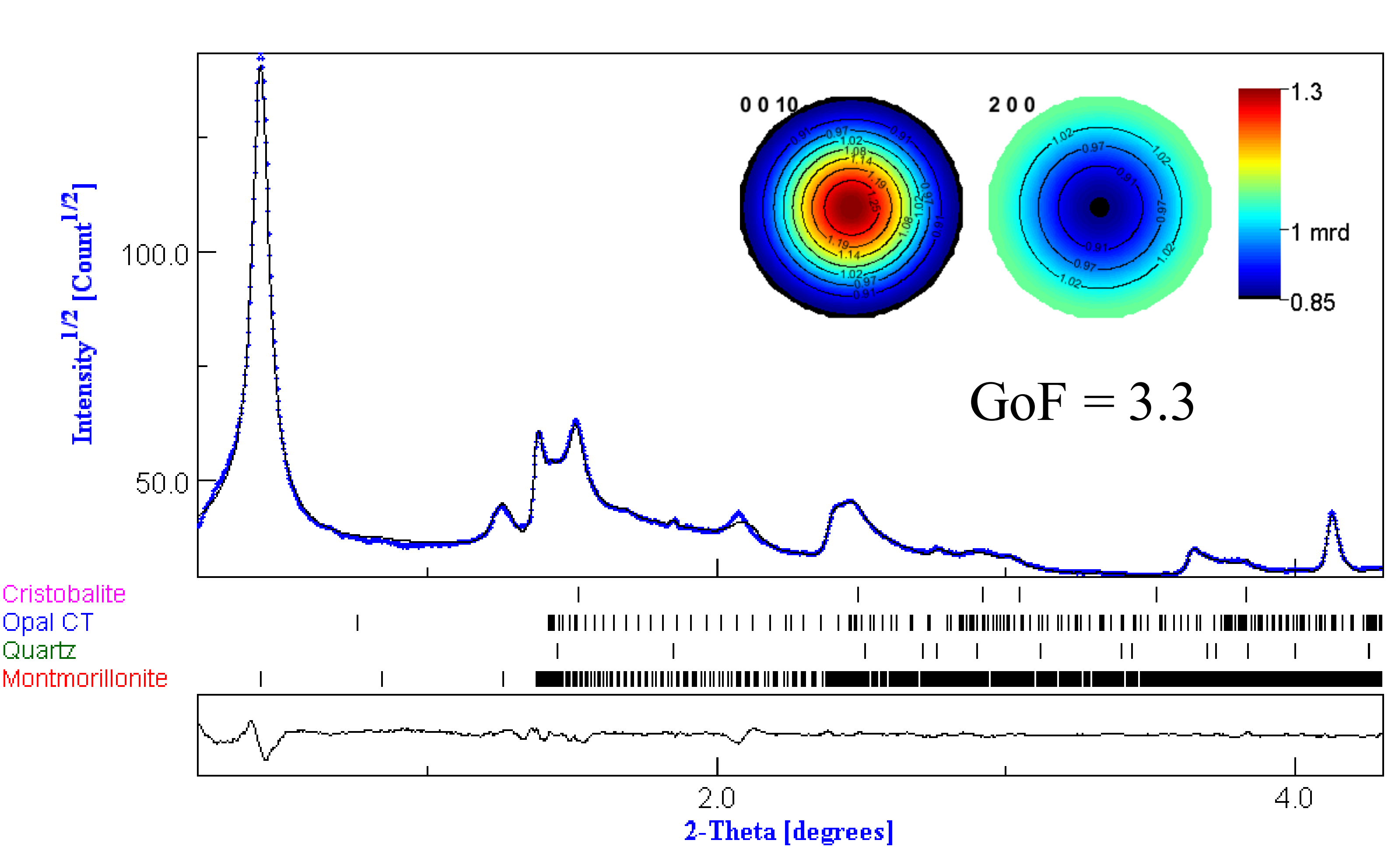

V%

1.45(2)

6.6(1)

0.19(1)

91.8(3)

$Mg_{0.75}Fe_{0.25}O$ high pressure experiments

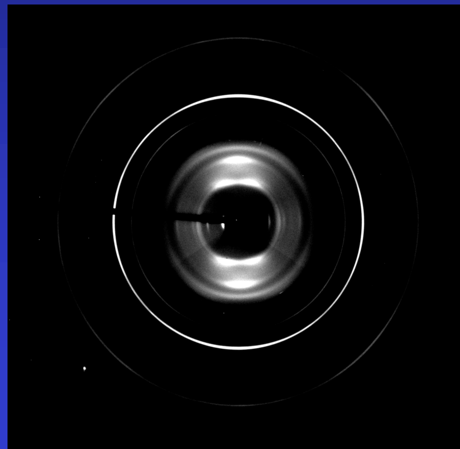

E-WIMV + geo

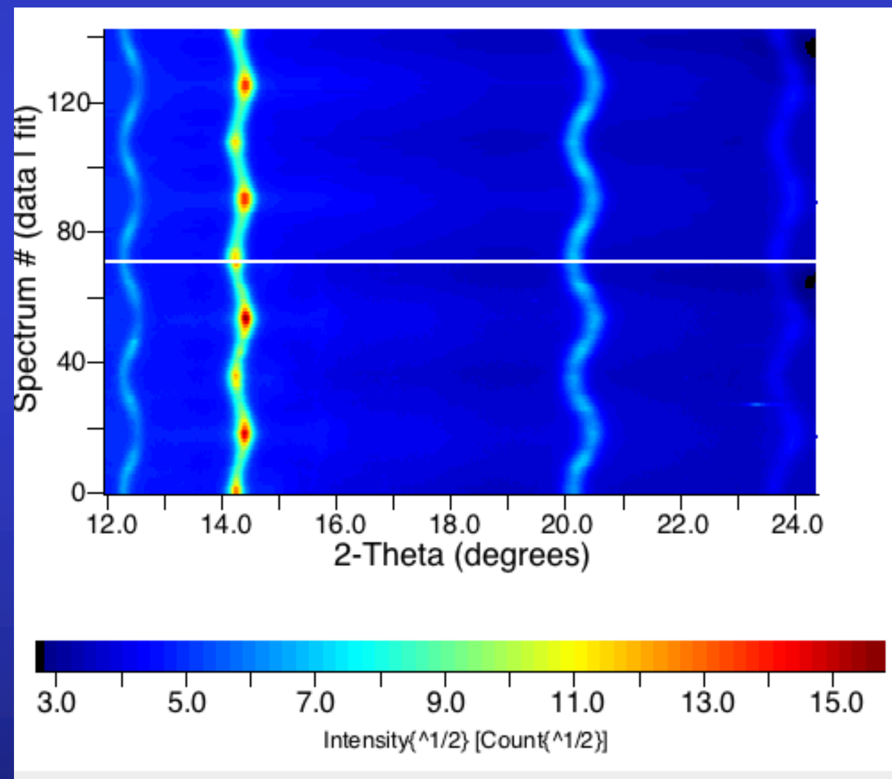

a = 3.98639(3) Å

<t> = 46.8(3) Å

$\langle\varepsilon\rangle$ = 0.00535(1)

σ_{33} = -861(3) MPa

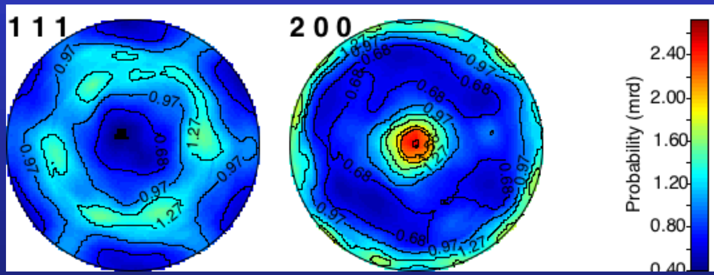

$LiNbO_3$

- Predict macroscopic anisotropic properties: BAW

Propagation equation

$$\rho \frac{\partial^2 u^i}{\partial t^2} = \left[C^{i\ell mn} \right] \frac{\partial^2 u_n}{\partial x^m \partial x^\ell}$$

Propagation direction	V_P	V_{S1}	V_{S2}
[100]	$\sqrt{\frac{c^M{}_{11}}{\rho}}$	$\sqrt{\frac{c^M{}_{44}}{\rho}}$	$\sqrt{\frac{c^M{}_{44}}{\rho}}$
[110]	$\sqrt{\frac{c^M{}_{11} + 2c^M{}_{44} + c^M{}_{12}}{2\rho}}$	$\sqrt{\frac{c^M{}_{11} - c^M{}_{12}}{2\rho}}$	$\sqrt{\frac{c^M{}_{44}}{\rho}}$
[111]	$\sqrt{\frac{c^M{}_{11} + 4c^M{}_{44} + 2c^M{}_{12}}{3\rho}}$	$\sqrt{\frac{c^M{}_{11} + c^M{}_{44} - c^M{}_{12}}{3\rho}}$	$\sqrt{\frac{c^M{}_{11} + c^M{}_{44} - c^M{}_{12}}{3\rho}}$

Cubic crystal system

	c_{11} or c_{11}^M	c_{12} or c_{12}^M	c_{13} or c_{13}^M	c_{14} or c_{14}^M	c_{33} or c_{33}^M	c_{44} or c_{44}^M
Single crystal	201	54.52	71.43	8.4	246.5	60.55
$LiNbO_3$/Si	206.4	68.5	67.6	0.48	216.5	64
$LiNbO_3/Al_2O_3$	204	65.7	69.7	1.1	219.9	63.2

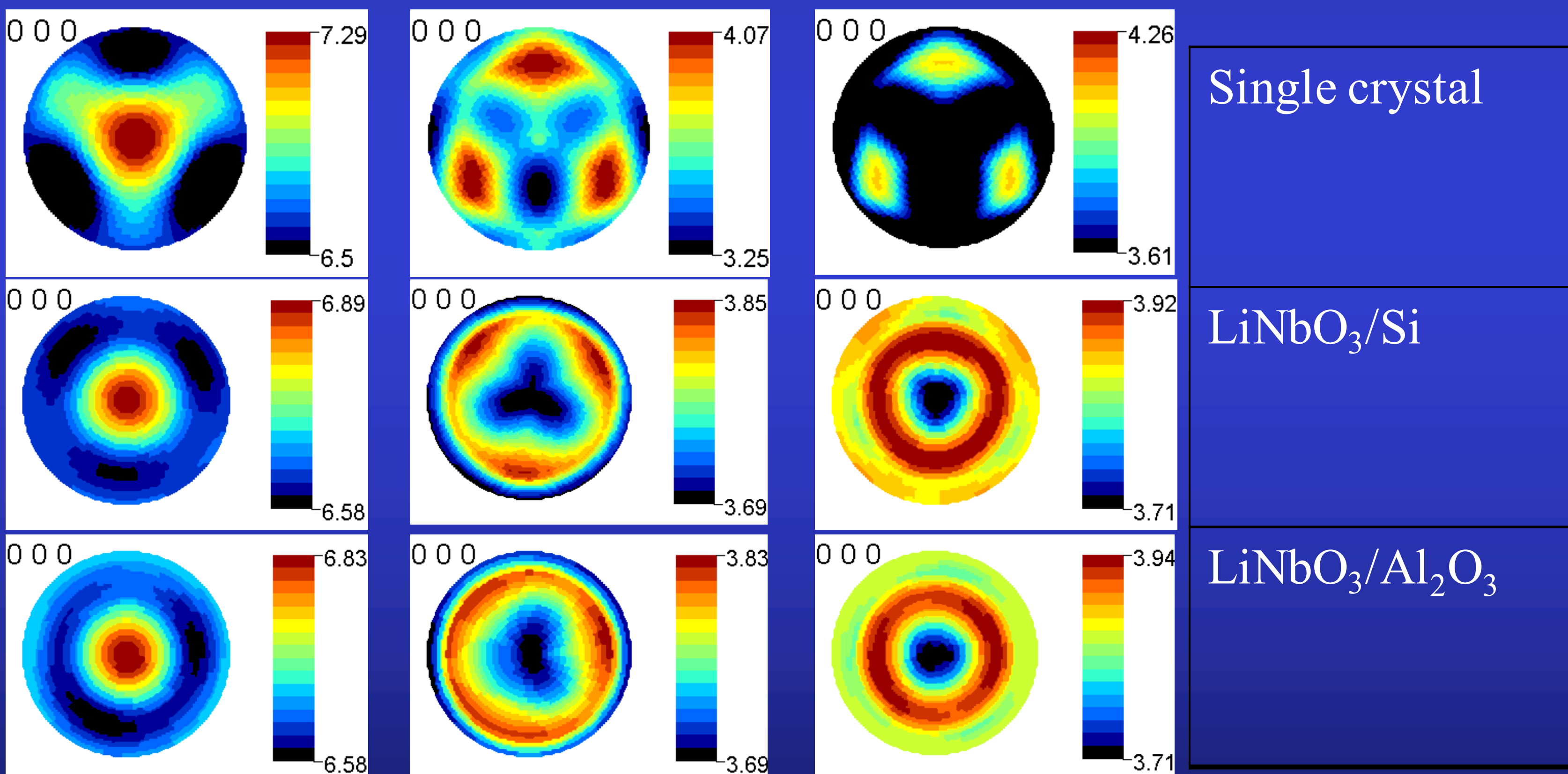

$ErMn_3Fe_9C$ ferrimagnet

Predict macroscopic anisotropic properties: Magnetisation

$$\frac{M_\perp}{M_S} = 2\pi\int_0^{\frac{\pi}{2}}(1-\rho_0)PV(\theta_g)\sin\theta_g\cos(\theta_g-\theta)\,d\theta_g + \rho_0 M_{random}$$

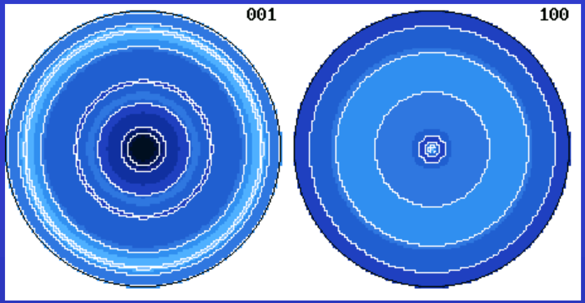

max {001}: 3.9 mrd
min: 0.5 mrd

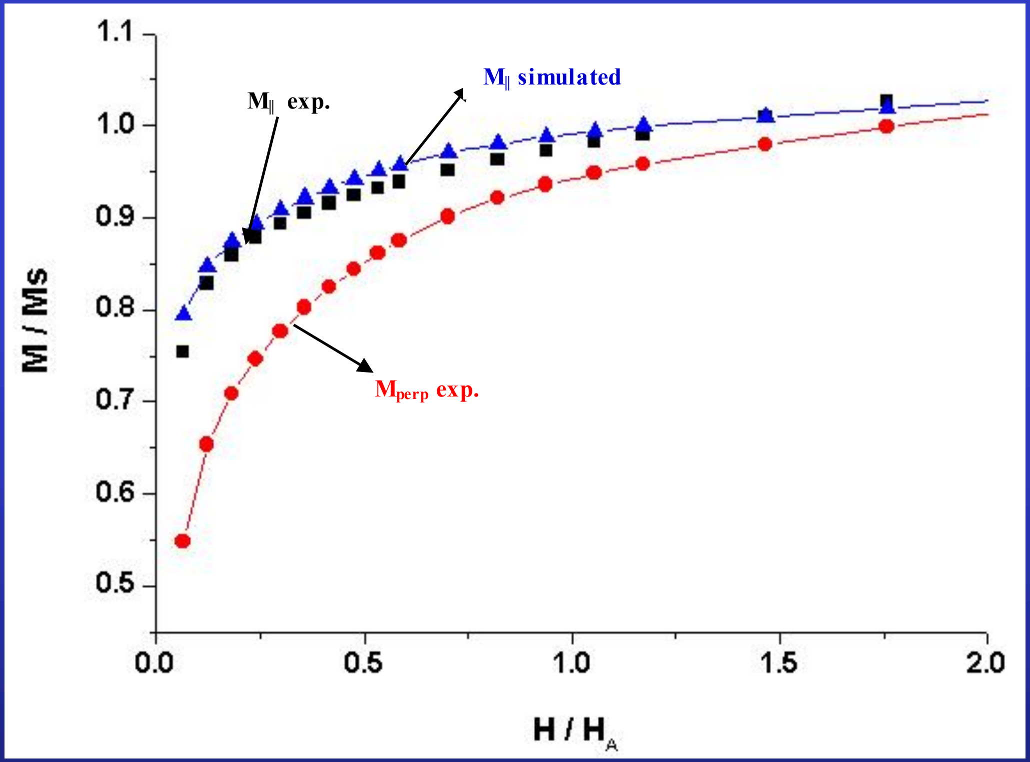

Combined XRR, XRD & GiXRF Analysis

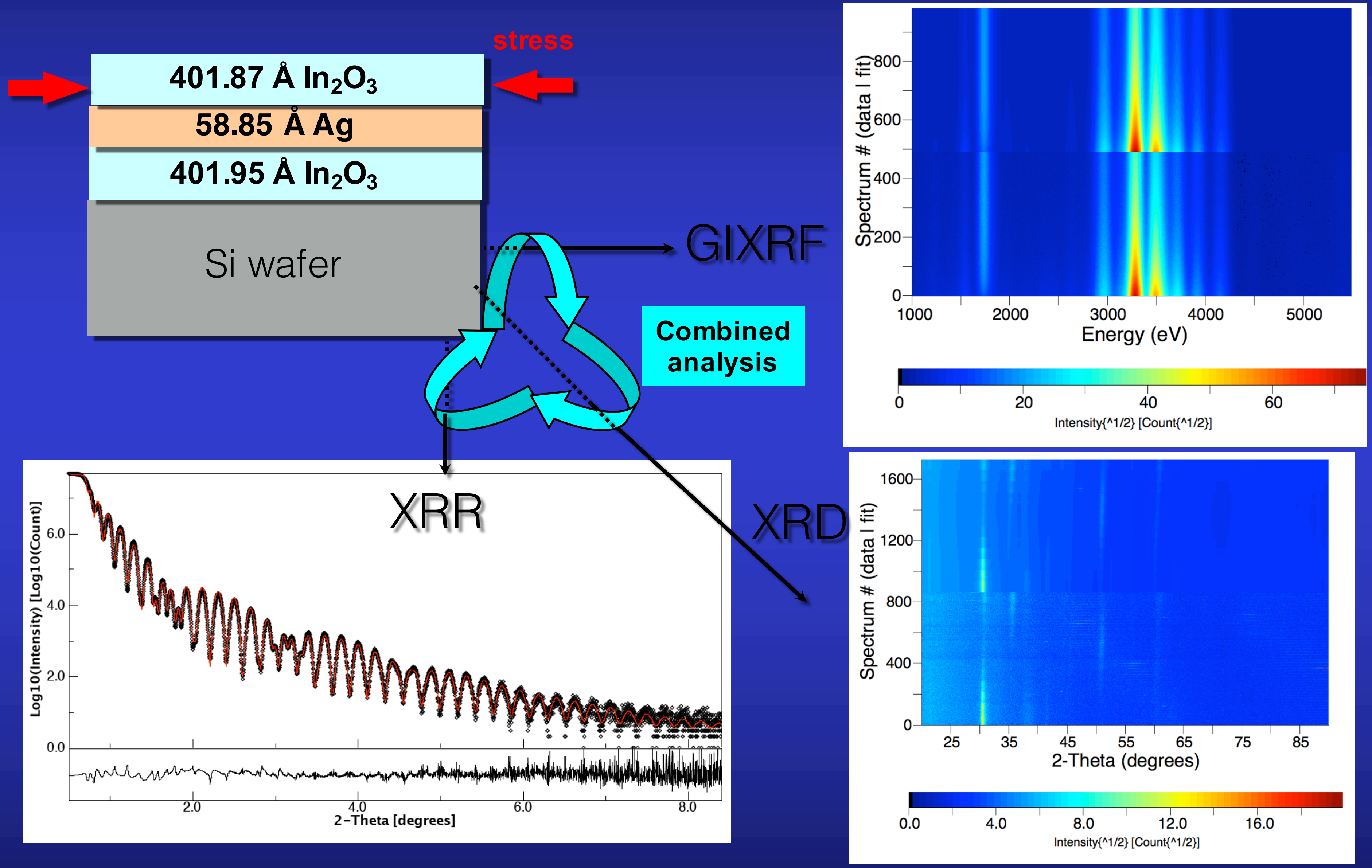

XRR

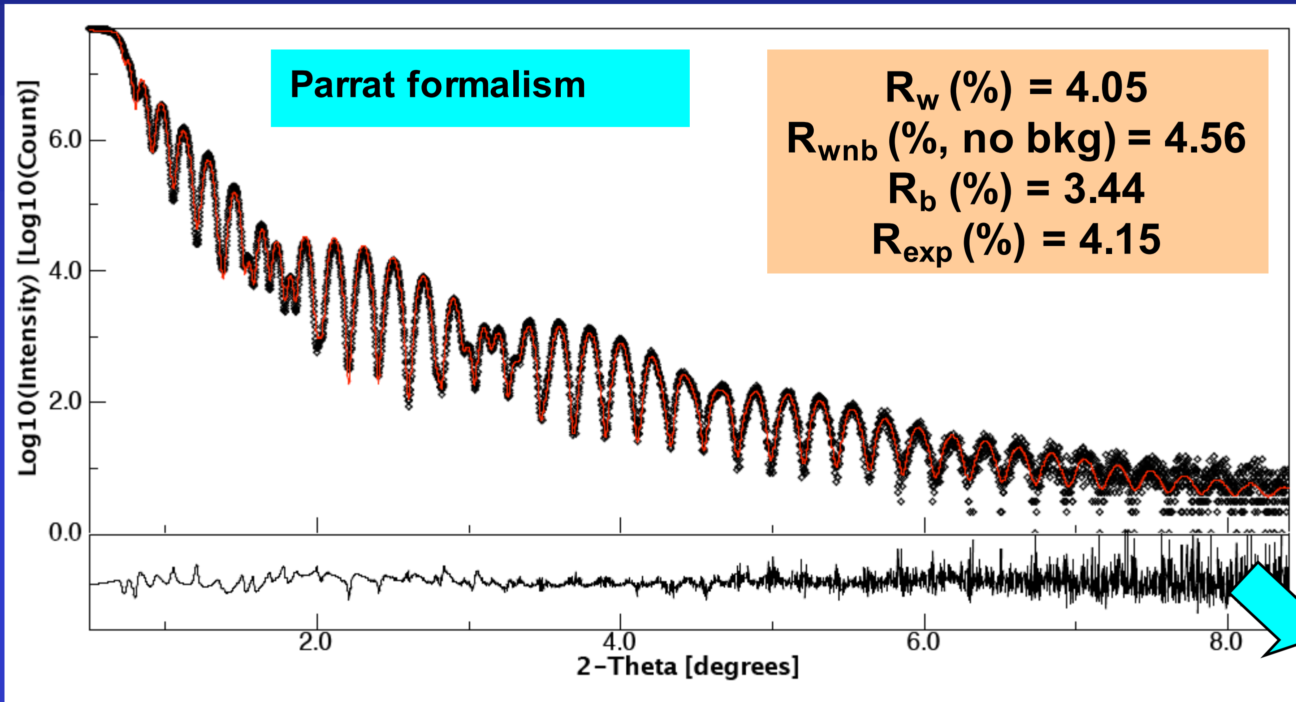

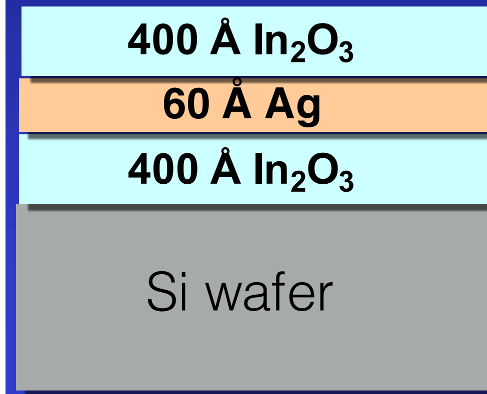

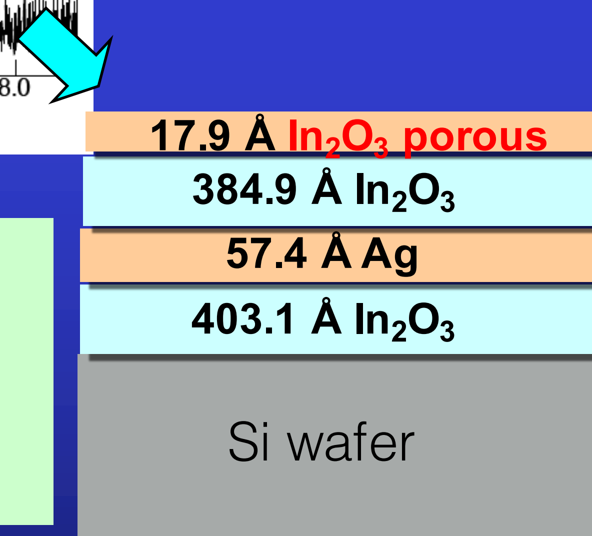

Highly porous In_2O_3 layer

Top layer: q_c = 0.0294 $Å^{-1}$; roughness r =0.38nm

Top In_2O_3: q_c = 0.0504 $Å^{-1}$; r =2.06 nm

Ag : q_c = 0.0576 $Å^{-1}$; r =0.26 nm

Bottom In_2O_3: q_c = 0.04889 $Å^{-1}$; r =6.74 nm

Si wafer: q_c = 0.0313 $Å^{-1}$; r = 0.73 nm

XRD

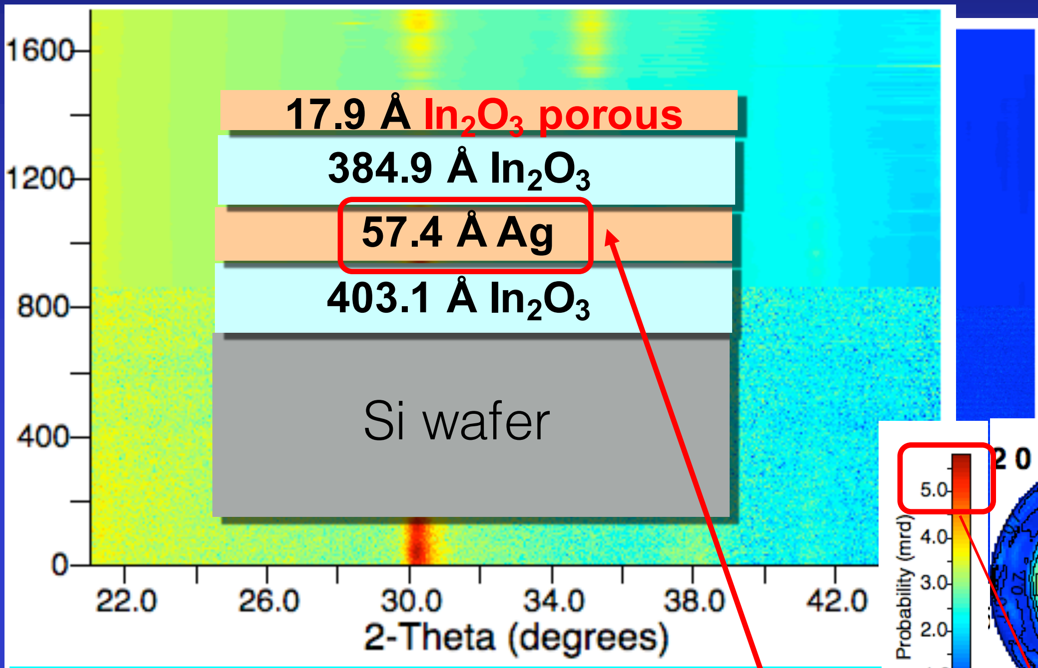

R_w (%) = 23.97
R_{wnb} (%, no bkg) = 58.31
R_b (%) = 18.71
R_{exp} (%) = 22.04

In_2O_3

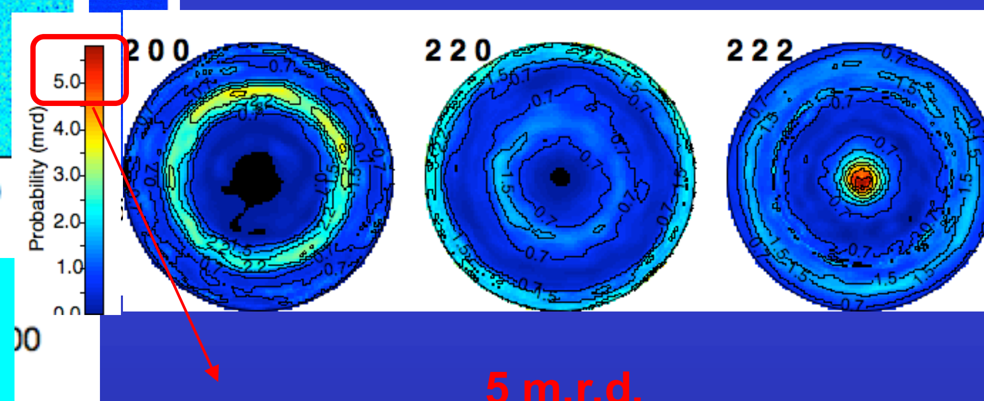

5 m.r.d.

Refined Ag phase parameters

- Isotropic crystallite size = 56.4 (1.3) Å
- Cell parameter: a = 4.0943(7) Å

Ag:

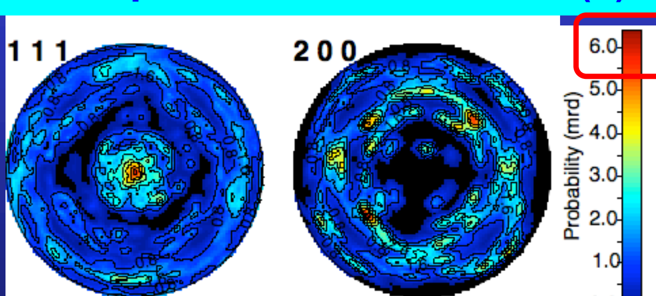

Refined In_2O_3 phase parameters

- σ_{XX} = - 1 GPa (in-plane compressive stress)
- Isotropic crystallite size = 153.2(5) Å
- Cell parameter: a = 10.2104(5) Å

GiXRF

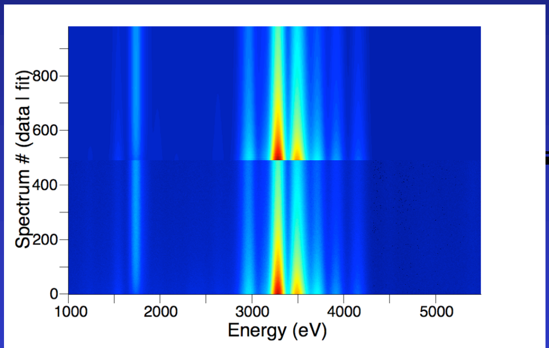

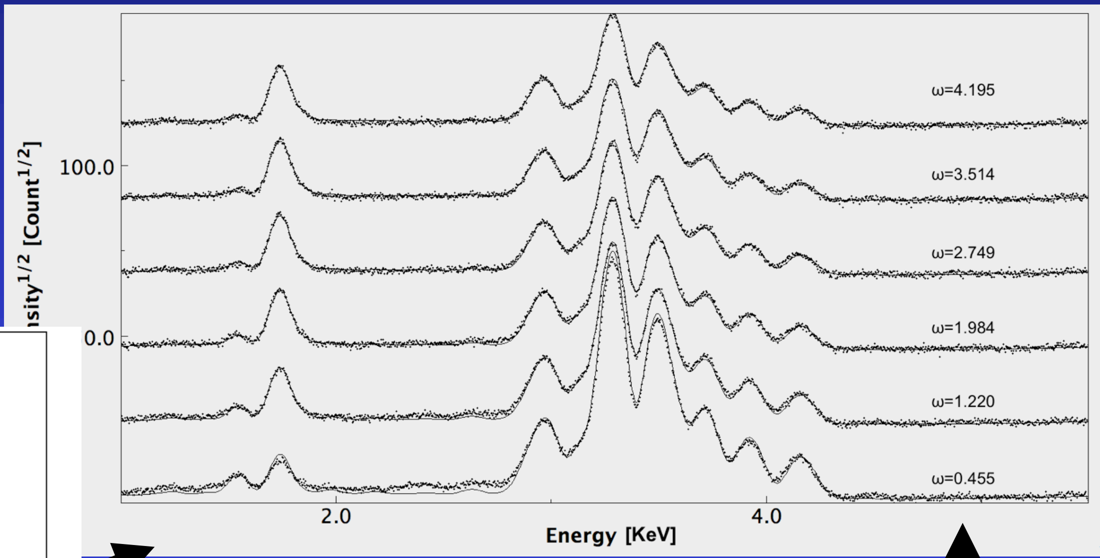

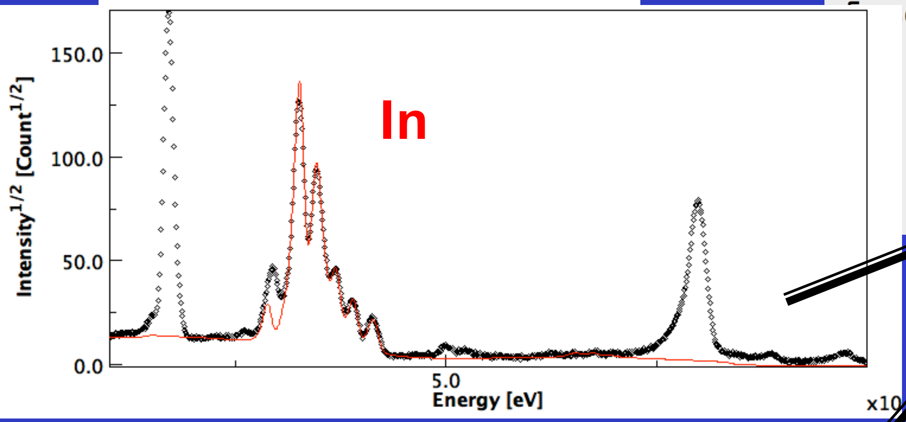

No presence of contaminant observed

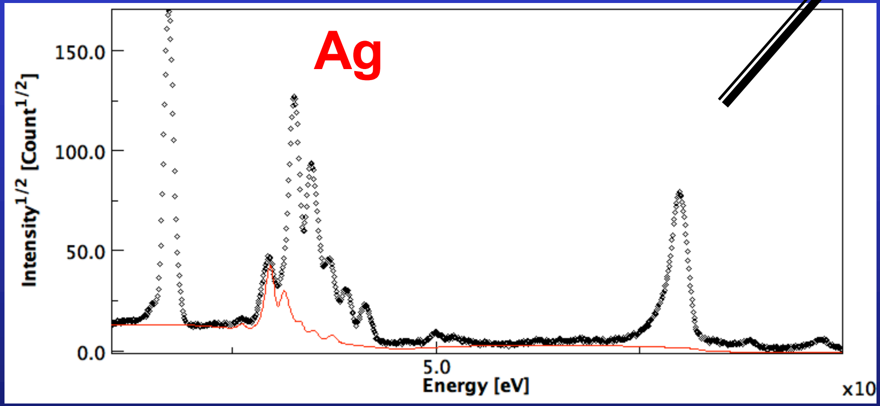

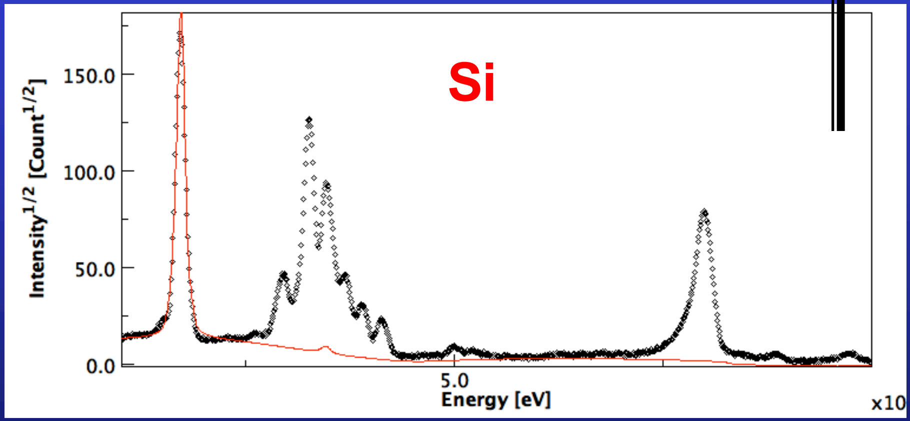

Magnetic QTA

$$I_{\vec{h}}(\vec{y},0) = I^{n}_{\vec{h}}(\vec{y},0) + I^{m}_{\vec{h}}(\vec{y},0)$$

$$I_{\vec{h}}(\vec{y},\vec{B}) = I^{n}_{\vec{h}}(\vec{y},0) + I^{m}_{\vec{h}}(\vec{y},\vec{B})$$

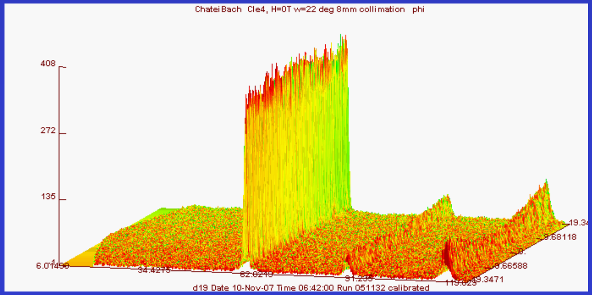

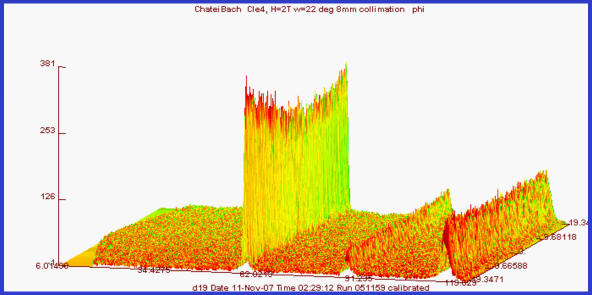

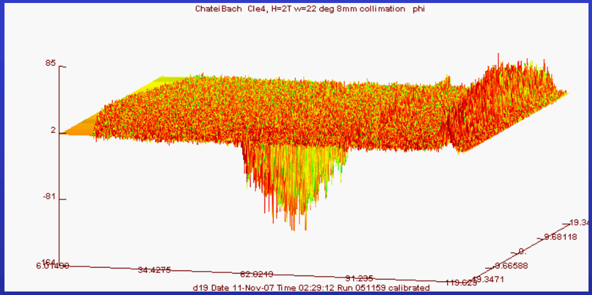

$$\Delta I^{m}_{\vec{h}}(\vec{y},\vec{B}) = I_{\vec{h}}(\vec{y},\vec{B}) - I_{\vec{h}}(\vec{y},0)$$

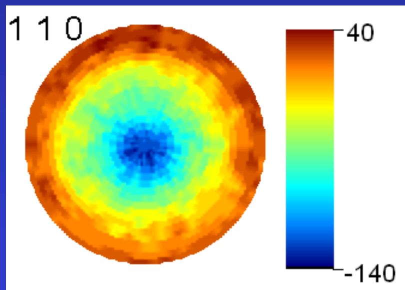

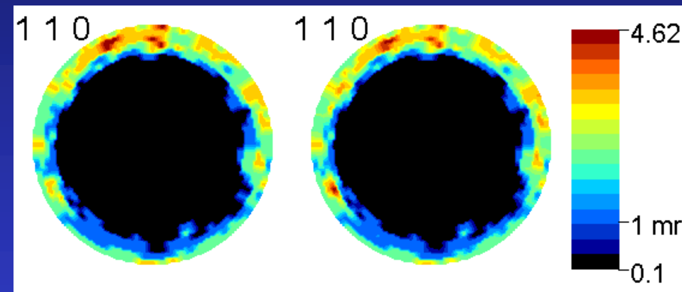

$$\Delta I^{+p}_{\vec{h}}(\vec{y},\vec{B})$$

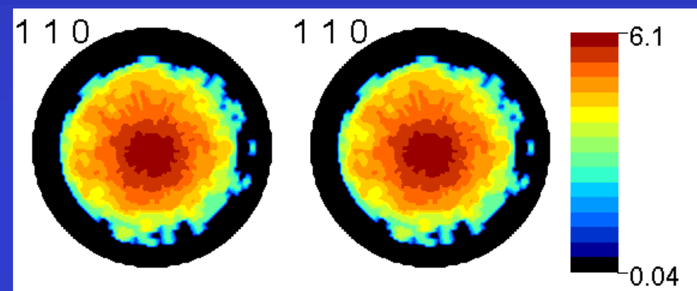

$$\Delta I^{-p}_{\vec{h}}(\vec{y},\vec{B})$$

$$P_h(y,\vec{B}) = \frac{1}{2\pi}\int_{h\|y} f_{n,m}(g)\,d\bar{\varphi}$$

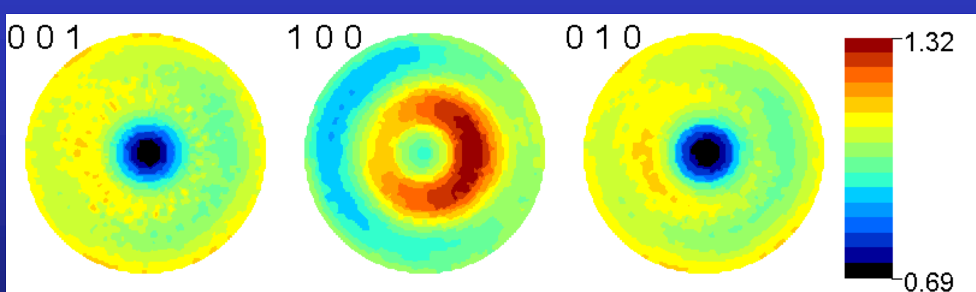

***** True iteration step #120 *****

ODF min max:	*0.64*	*2.26*
Texture Index (F^2)	*1.029*	
Entropy	*-0.014*	
Average RP	*0.24*	
Average RP1	*0.30*	

More ?

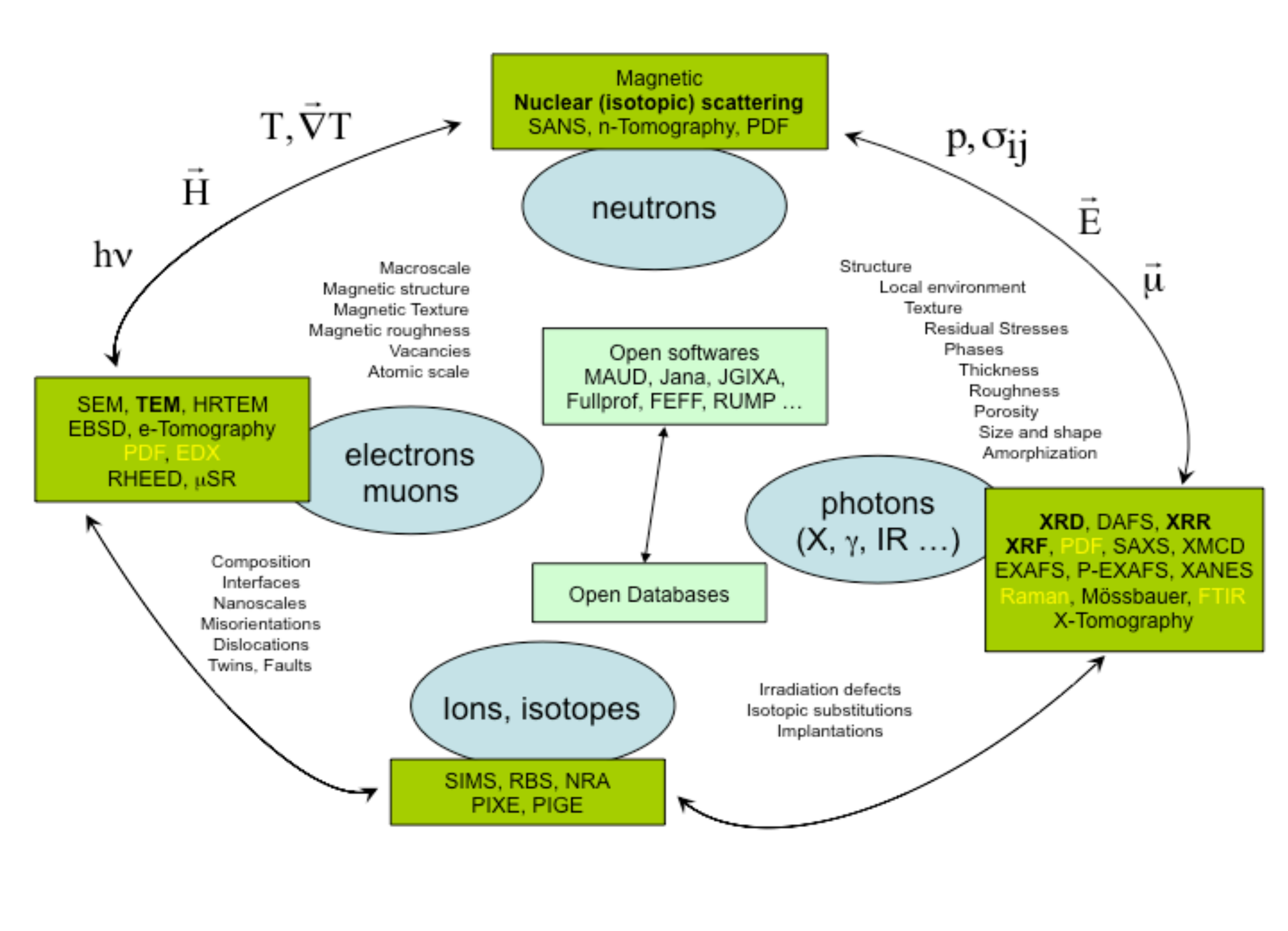

Magnetic
Nuclear (isotopic) scattering
SANS, n-Tomography, PDF
neutrons
T, ∇T
H
hν
p, σij
E
μ
Macroscale
Magnetic structure
Magnetic Texture
Magnetic roughness
Vacancies
Atomic scale
Structure
Local environment
Texture
Residual Stresses
Phases
Thickness
Roughness
Porosity
Size and shape
Amorphization
Open softwares
MAUD, Jana, JGIXA,
Fullprof, FEFF, RUMP …
SEM, TEM, HRTEM
EBSD, e-Tomography
PDF, EDX
RHEED, μSR
electrons
muons
photons
(X, γ, IR …)
XRD, DAFS, XRR
XRF, PDF, SAXS, XMCD
EXAFS, P-EXAFS, XANES
Raman, Mössbauer, FTIR
X-Tomography
Open Databases
Composition
Interfaces
Nanoscales
Misorientations
Dislocations
Twins, Faults
Ions, isotopes
Irradiation defects
Isotopic substitutions
Implantations
SIMS, RBS, NRA
PIXE, PIGE

Combined Measurement-Analysis for SOLSA

Sequential Acquisition (on-mine real-time)

Hyperspectral
3D imaging

XRD XRF Raman IR

Sonic
drilling

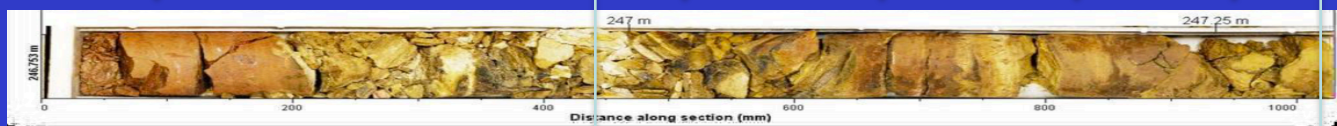

ID2A and B

Conveyor

Global XRD-XRF-Raman-IR
Full-Profile Search-Match
QPA – chemical analysis

Open Databases:
COD
TCOD
ROD …

Combined Analysis

or Combined Measurements and Analysis: → ID1

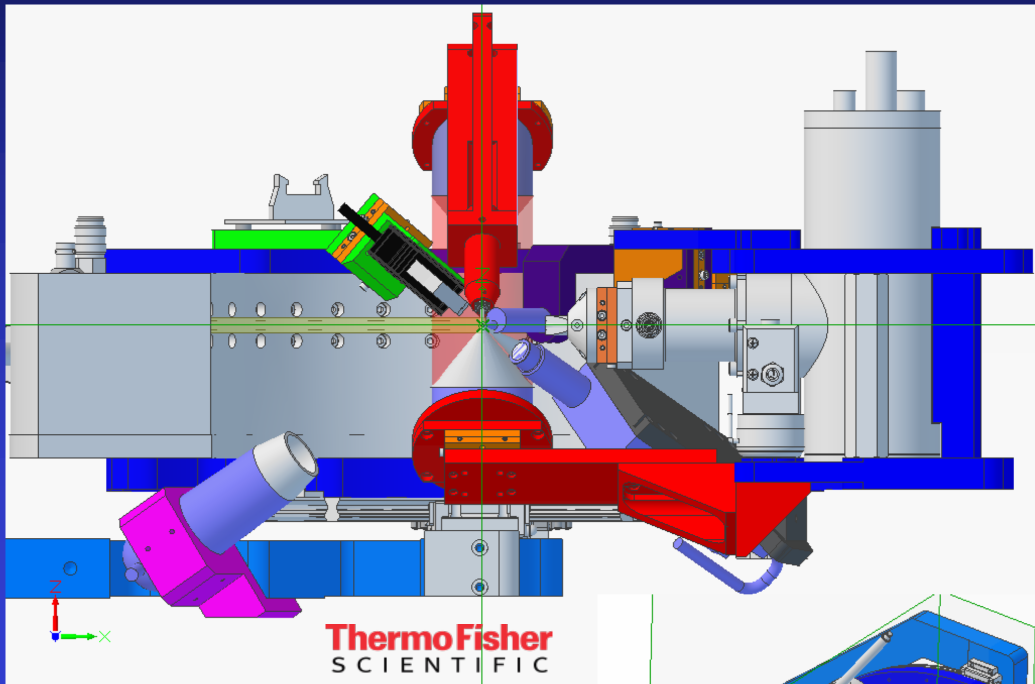

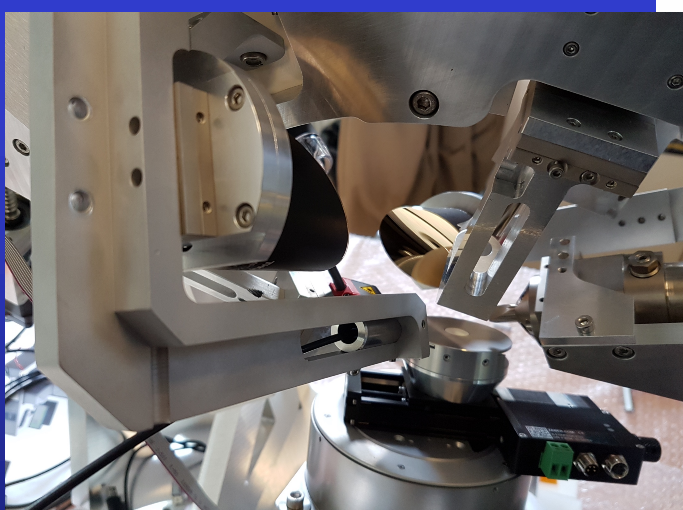

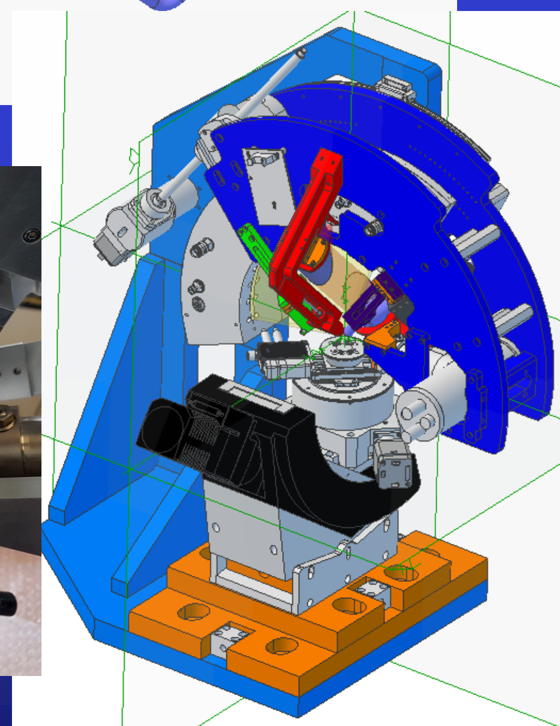

XRD-XRF-Raman-FTIR Combined Analysis (SOLSA EU projet)

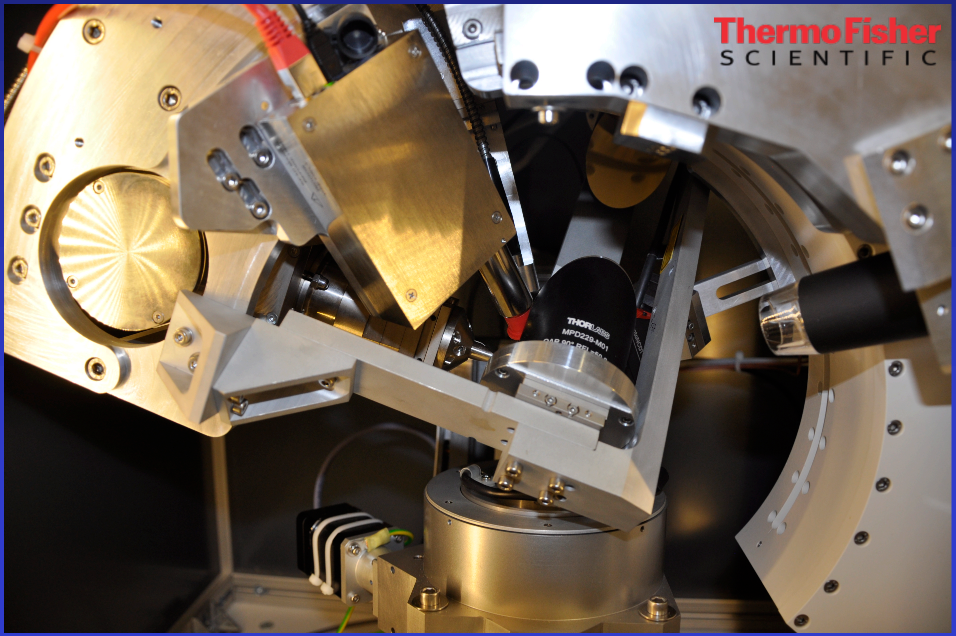

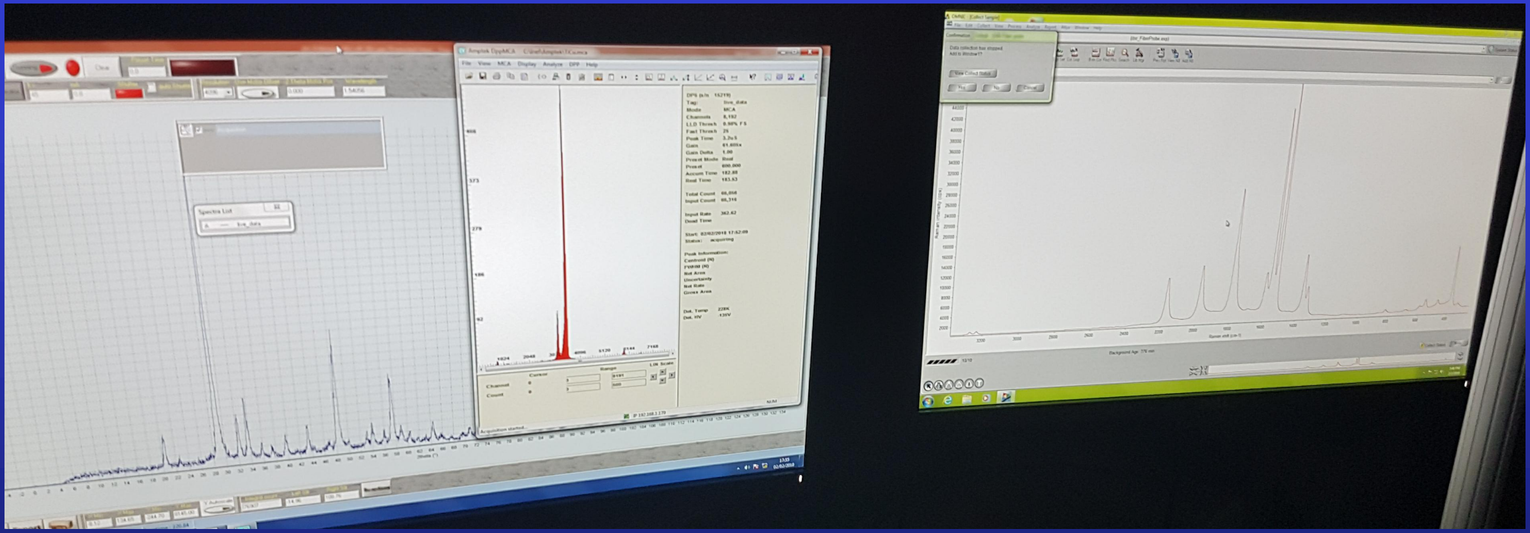

XRD-
XRF-
Raman

Comb.
Meas.

XRD-XRF-Raman-IR Combined Analysis

$$I_{aj} = \frac{\lambda}{hc} C_{aj} \frac{\tau_{aj}}{\mu_{j\lambda}/\rho_j} J_{aj}\omega_a g_a exp\left\{-\sum_{n=1}^{j-1}\frac{\mu_{na}d_n}{sin\Psi_d}\right\} S_1 \int_0^{d_j} dz \left(\frac{-\partial P_{jz}}{\partial z}\right) exp\left(\frac{\mu_{ja}z}{sin\Psi_d}\right)$$

IR

XRF-GiXRF- TXRF
EDS

Databases
COD-ROD-MPOD

Raman

$$I_{(e_s,e_0)} = I_0 \frac{\hbar}{2\omega_m}(n_m+1)\frac{(\omega_0-\omega_m)^4}{c^4}\left|e_s.\alpha_{ij}^m.e_0\right|^2$$

XRR

$$r = \frac{M_{12}}{M_{22}} = \frac{r_{01}+r_{12}e^{-2iq_{1z}h}}{1+r_{01}r_{12}e^{-2iq_{1z}h}}$$

Diffraction extended Rietveld (n, X, e^-)

$$y_c(\mathbf{y_S},\theta,\eta) = y_b(\mathbf{y_S},\theta,\eta) + I_0\sum_{i=1}^{N_L}\sum_{\Phi=1}^{N_\Phi}\frac{\nu_{i\Phi}}{V_{c\Phi}^2}\sum_h Lp(\theta) j_{\Phi h}\left|F_{\Phi h}\right|^2 \Omega_{\Phi h}(\mathbf{y_S},\theta,\eta) P_{\Phi h}(\mathbf{y_S},\theta,\eta) A_{i\Phi}(\mathbf{y_S},\theta,\eta)$$

Full-Pattern Search-Match

http://nanoair.dii.unitn.it:8080/sfpm/
cod.iutcaen.unicaen.fr

Diffraction pattern and sample composition

Upload diffraction pattern: [ ] Parcourir...

Atomic elements in the sample: O Al Ca F Zn

☐ Sample nanocrystalline

Experiment details

Radiation:
◉ X-ray tube: Cu
○ Other : x-ray Wavelength (Å): 1.540598

Instrument geometry:
◉ Bragg-Brentano (theta-2theta)
○ Bragg-Brentano (2theta only), omega: 10
○ Debye-Scherrer
○ Transmission

Instrument broadening function: Medium

Search and quantify

☐ Extra output (for debugging)

Structures database: CODstructures

1 min later
>275000 COD structures

Found phases and quantification:

Phase ID	name	vol. (%)	wt. (%)	crystallites (Å)	microstrain
9004178	Zincite	16.8284	23.9708	2148.26	0.00028435
9009005	Fluorite	42.5522	33.9388	2117.08	0.000363147
9007498	Corundum	37.2197	37.2493	1889.82	0.000267779
2300112	zinc_oxide	3.39971	4.84114	1754.74	6.98311e-05

Final Rietveld analysis, Rw: 0.159468, GofF: 1.95869

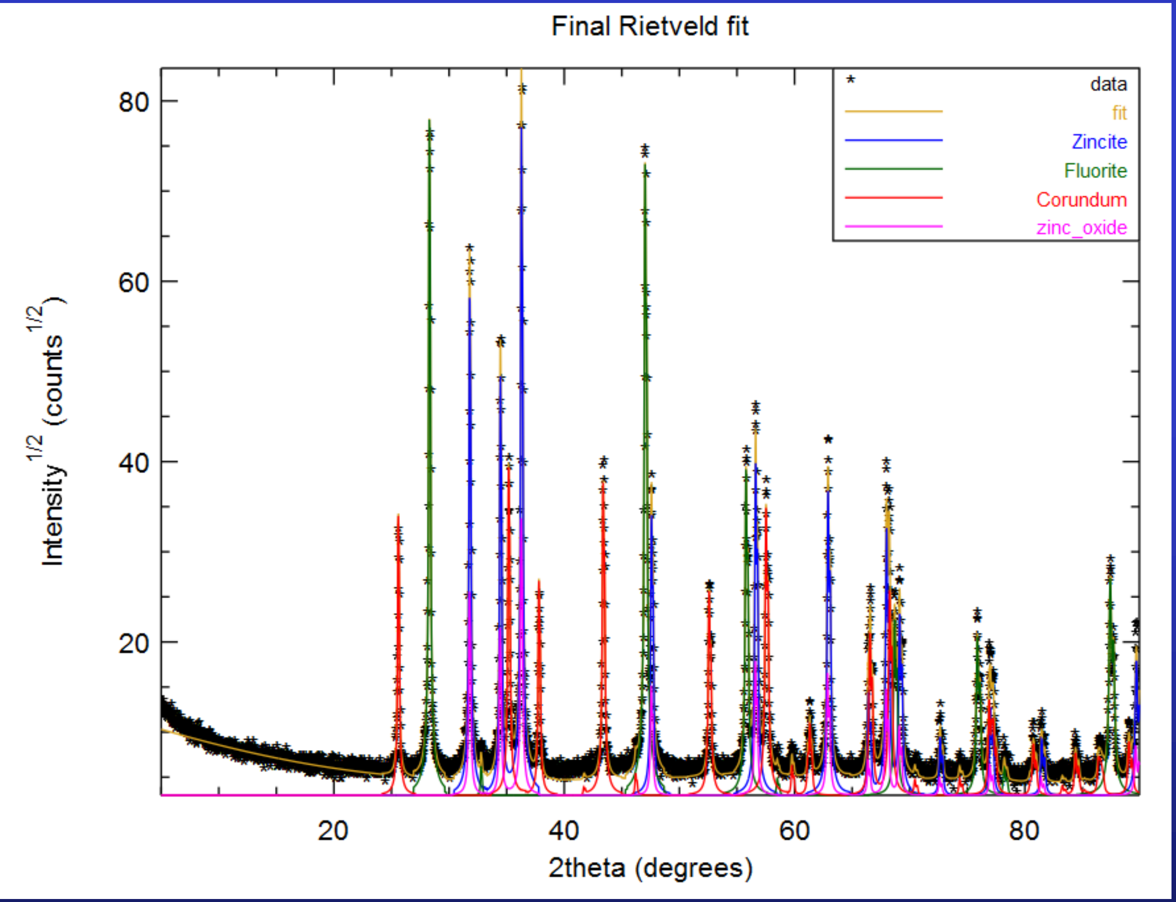

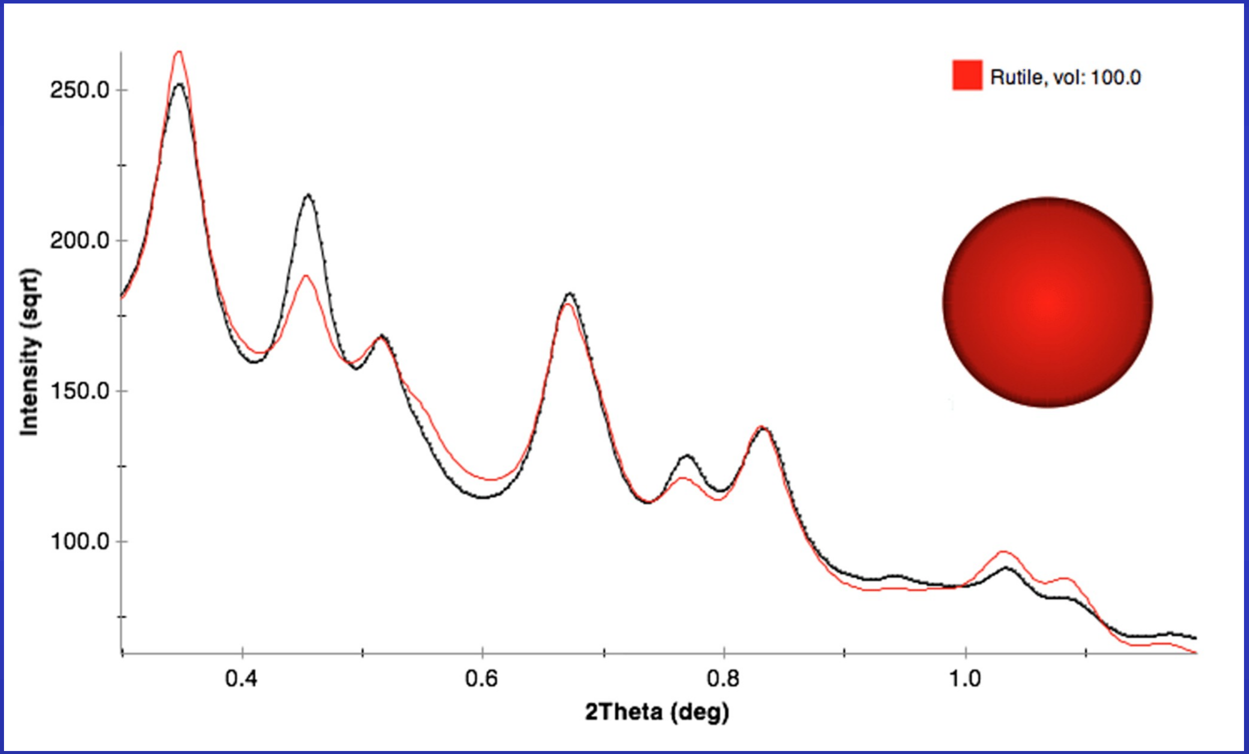

Rutile nanocrystalline Electron Powder Diffraction pattern

Combined Analysis Workshop series:

www.ecole.ensicaen.fr/~chateign/formation/

Thanks !

UNION EUROPENNE

ESQUI
SOLSA

MEET
MIND
Xmat
COSTs

l'Europe s'engage en Basse-Normandie avec le FEDER

COMBIX: Chair of Excellence

AGENCE NATIONALE DE LA RECHERCHE ANR

FURNACE
ECOCORAIL

DAME
SEMOME

Région Centre

SMAM